AIMS Mathematics, 10(2): 4000–4039.
DOI:10.3934/math.2025187
Received: 22 November 2024
Revised: 08 February 2025
Accepted: 18 February 2025
Published: 27 February 2025

https://www.aimspress.com/journal/Math

Research article

Analysis of a mathematical model for the spreading of the monkeypox virus with constant proportional-Caputo derivative operator

Jutarat Kongson[1], **Chatthai Thaiprayoon**[1] **and Weerawat Sudsutad**[2,*]

[1] Research Group of Theoretical and Computational Applied Science, Department of Mathematics, Faculty of Science, Burapha University, Chonburi 20131, Thailand

[2] Department of Statistics, Faculty of Science, Ramkhamhaeng University, Bangkok 10240, Thailand

* **Correspondence:** Email: weerawat.s@rumail.ru.ac.th.

Abstract: This work comprehensively analyzed the monkeypox virus utilizing a deterministic mathematical model within a constant proportional-Caputo derivative framework. The suggested model considered the interplay of human and rodent populations by incorporating certain realistic vaccination parameters. Our study was a testament to the thoroughness of this work. We explored the uniqueness result using Banach's contraction principle. The solution's positivity and boundedness were studied in detail, as were the basic reproduction number and the stability analysis of the system's equilibrium conditions. We performed a variety of Ulam's stability analyses to guarantee the solution existed. Additionally, we implemented a decomposition formula to obtain the numerical scheme. This numerical approach allowed for numerical simulation as a graphical representation for certain real data sets and different parameter values in order to understand the model's dynamic behavior.

Keywords: monkeypox disease; constant proportional-Caputo; Ulam stability; numerical algorithm; basic reproduction number
Mathematics Subject Classification: 26A33, 34A08, 65L09, 92D25, 92D30

1. Introduction

Presently, people in many countries face a series of epidemics, each caused by a different type of emerging or reemerging virus. Monkeypox (MPOX) disease is one of these urgent situations that need to be monitored appropriately since the World Health Organization (WHO) has recently reported a resurgence of the MPOX outbreak, with the disease reemerging and spreading across multiple countries worldwide. Numerous cases and clusters have been identified simultaneously in diverse geographical areas [1]. The MPOX virus is the cause of a zoonotic illness. The spreading of this virus to humans mainly comes through bites or scratches from wild animals, such as rodents and primates. Human-

to-human transmission arises through respiratory droplets or contact with body fluids when a person touches a lesion on an infected individual or their items. The symptoms of MPOX patients frequently resemble those of smallpox but are less severe. It begins with a slight fever, chills, weariness, muscle aches, exhaustion, and headache. The MPOX can cause swelling in the lymph nodes, while smallpox does not cause lymphadenopathy. The time between the onset of symptoms and the rash completely recovering typically lasts 14–28 days [2–4]. Currently, there is no vaccine that directly protects against MPOX disease. However, due to the similarity between the virus that causes MPOX disease and smallpox disease, vaccination against smallpox is the best choice. It effectively prevents MPOX disease by as much as 80–85 percent [5]. Mathematical models of epidemics have long been used to help us understand the effects of numerous disease transmissions in the real world. Understanding the virus and its transmission dynamics is critical for establishing efficient prevention and control strategies. Therefore, many researchers have focused on developing the MPOX epidemic model for various reasons, including potential human outbreaks. Some examples of interesting works, such as the analysis of the MPOX disease with the impact of vaccination, were studied in [6, 7] A quarantine class and an enlightenment campaign were incorporated into the MPOX model, which can be found in [8], while the factor of isolated humans was added to the model, as seen in [9–11]. In [12], pox-like analysis was investigated under the factor of recovery with permanent immunity. Monkeypox analysis using data and statistical tools were examined in [13, 14].

Fractional calculus is an area of pure mathematics that generalizes the concepts of differentiation and integration involving non-integer derivatives and integrals. It is a valuable and efficient tool for describing complex dynamical systems and simulating real-world problems, particularly in epidemiology, since it has hereditary properties and describes memory in the context of numerous diseases. Besides, fractional models provide a more realistic illness trajectory. Fractional differential operators enhance epidemiological modeling by combining memory, heterogeneity, and nonlocal dynamics. This leads to more accurate predictions, a better understanding of diseases, and improved control strategies for illnesses such as monkeypox, COVID-19, HIV, and so on. Fractional derivatives, which can take any real number as an order, are highly flexible and nonlocal. These characteristics make them more dependable than classical derivatives for approximating real data since they take into account global interactions and memory effects. Researchers have defined the many forms of fractional derivative operators in fractional calculus. Each form is created to capture distinct characteristics of the fractional derivative idea. For instance, Riemann-Liouville ($\mathbb{RL}$, one of the original definitions of fractional derivative), Caputo [15, 16], Caputo-Katugampola [17], Caputo-Fabrizio [18, 19], Atangana-Baleanu [18, 19], Hilfer [20], constant proportional-Caputo ($\mathbb{CPC}$) [21], and (k, ψ)-Hilfer proportional [22]. The $\mathbb{CPC}$ derivative is a modern development in the fractional derivative, which is designed in [21]. It is a hybrid concept between Caputo's type and the proportional derivatives to gain a novel type of fractional calculus and potential applications for modeling actual data from various problems. In addition, the $\mathbb{CPC}$ operator is a more comprehensive framework than the Caputo fractional derivative operator, for which supporting research can be found in [23, 24]. This operator offers a significant advantage by effectively addressing current challenges in different issues that traditional operators cannot adequately evaluate. Several studies [25–27] highlight that the $\mathbb{CPC}$ operator provides a more practical and accurate approach for examining mathematical models applied to real-world problems using real data compared to classical and fractional-order operators.

The application of fractional calculus to mathematical modeling is a novel approach that has

captured the interest of many researchers across diverse scientific domains. It is particularly intriguing due to the memory effect, a unique and powerful characteristic of fractional-order models, which remains supereminent over the classical models due to the diverse properties of fractional operators that yield more accurate and reliable data. Many fractional models consist of differential equations carefully designed by researchers to address the pressing problems within the global environment. Extensive research has been conducted on studying and analyzing fractional-order models for disease transmission dynamics. El-Mesady et al. [28] designed a fractional-order vaccination mathematical model for tuberculosis incorporating a susceptible class with an underlying ailment. Peter et al. [29] developed a fractional mathematical model for studying measles infection with double-dose vaccination. The work [30] constructed a mathematical model under the Atangana-Baleanu-Caputo derivative to examine meningitis with treatment and vaccination dynamics. The authors [31] presented the pneumococcal pneumonia infection model using fractional-order derivatives in the sense of the Caputo-Fabrizio operator. Peter [32] studied the transmission dynamics of a Brucellosis model under the Caputo-Fabrizio fractional operator. Additionally, $\mathbb{MPOX}$ virus infection is one of the research areas that has gotten a lot of attention and produced some fascinating results since the disease resurfaced after a long hiatus. We refer the reader to several previously interesting works about the $\mathbb{MPOX}$ fractional model. For example, Peter et al. [33] presented and established the dynamical behavior of the $\mathbb{MPOX}$ virus model by using both classical and differential equations via the Caputo-Fabrizio fractional derivative. Ngungu et al. [34] studied the dynamics of the $\mathbb{MPOX}$ virus spreading with a non-pharmaceutical intervention using real-time data with the Caputo-Fabrizio operator. Wireko et al. [35] used fractal-fractional operators ($\mathbb{FFO}s$) to explore the biological behavior of the $\mathbb{MPOX}$ disease. Sudsutad et al. [36] investigated the theoretical analysis for the transmission of the $\mathbb{MPOX}$ virus fractional model under the $\mathbb{FFO}s$ involving the Atangana-Baleanu sense. The study by El-Mesady et al. [37] looked into how the $\mathbb{MPOX}$ virus spreads in human hosts and rodent populations using a Caputo fractional-order nonlinear model. The $\mathbb{MPOX}$ virus is established by applying a deterministic mathematical model in the context of the Atangana-Baleanu fractional derivative that depends on the generalized Mittag-Leffler kernel [38]. Zhang et al. [39] studied a deterministic Caputo fractional-order mathematical model of Marburg-$\mathbb{MPOX}$ virus co-infection transmission. Liu et al. [40] analyzed the dynamics of a $\mathbb{MPOX}$ disease with the impact of vaccination utilizing a fractional mathematical model. For more works, we refer readers to see [41, 42]. However, even though many researchers employ fractional differential systems to understand real-world phenomena, finding exact solutions to such systems through manual methods is still a formidable challenge. Hence, several efficient techniques are produced to find the approximated solution of fractional differential systems, such as the predictor-corrector [43, 44], Adams-Bashforth [43, 45], Newton polynomial [43, 45], and the decomposition formula method [46,47]. The last introduced powerful knowledge is Ulam stability, an essential technique in mathematical analysis and other related sciences. Ulam stability is vital to maintaining the stability and reliability of solutions under minor variations. It ensures that solutions remain valid and usable even though conditions change marginally. There are various kinds of Ulam stability commonly used, like Ulam-Hyers ($\mathbb{UH}$) stability and Ulam-Hyers-Rassias ($\mathbb{UHR}$) stability; see the history and its application in [48–51].

After composing all of the stories and being motivated by the above discussions, the $\mathbb{CPC}$ operator is particularly interesting in this aspect because it is a recent operator, and there has been little literature-based research on its application. Also, to the best of our current understanding, no studies using

the proposed derivative operator have been conducted or published in the existing literature on the dynamics of the monkeypox virus as well as the benefit of using the $\mathbb{CPC}$ operator, as mentioned above, to address memory and hereditary properties for resulting in more accurate prediction and translation. Therefore, this study takes a comprehensive approach to analyzing the behavior of the $\mathbb{MPOX}$ model and investigating the factors influencing population changes, which may help control the monkeypox outbreak. We have developed a deterministic $\mathbb{MPOX}$ model by extending the works [9, 33] in terms of incorporating the vaccinated-individuals compartment into the model and yielding a unique classical model. Later, we transform the model into a fractional-order system using the $\mathbb{CPC}$ operator to gain a better understanding of the virus dynamics. Our focus is on studying the dynamic behavior of this model, a task we accomplish by leveraging the well-known fixed-point theory of Banach's type to prove the solution's existence and uniqueness. We investigate the stability of equilibrium points with the help of the basic reproduction number. Moreover, we ensure the solutions exist by analyzing their stability via various Ulam stability. A decomposition formula for the $\mathbb{CPC}$ derivative technique is derived to obtain the numerical scheme, and some graphics in the numerical simulation are shown to visualize the system's behavior analysis. This work will help to fill the gap in the study of monkeypox transmittance using fractional derivatives and expand the scope of this study to benefit disease control.

The remaining sections of the paper are as follows: Section 2 introduces some concepts of the $\mathbb{CPC}$ operators. The $\mathbb{MPOX}$ model construction is presented in Section 3. Section 4 is dedicated to investigating model analysis, including the solution's positiveness and boundedness, the basic reproduction number, and the local stability analysis of the equilibrium points. Section 5 explores the existence theory for the proposed model; that is, the uniqueness result is verified using Banach's fixed-point theorem. Section 6 verifies various Ulam's type stability and their generalization. The numerical scheme derived from a decomposition formula for the $\mathbb{CPC}$ derivative is determined in Section 7. Finally, the results are discussed via some examples, and the summation of this discussion is given in the final part.

2. Preliminaries

This section provides some fundamental definitions and properties of fractional calculus, which will be used to analyze the system throughout this work.

Definition 2.1. ([52]). *The Caputo fractional order derivative of a function f with order $\alpha \in (0, 1)$ is provided by*

$$^{\mathbb{C}}\mathfrak{D}^{\alpha}_{0,t} f(t) = \frac{1}{\Gamma(1-\alpha)} \int_0^t f'(s)(t-s)^{-\alpha} ds.$$

Definition 2.2. ([52]). *Assume $f(t)$ is an integrable function. The $\mathbb{RL}$-integral of $\alpha > 0$ is given by*

$$^{\mathbb{RL}}\mathcal{I}^{\alpha}_{0,t} f(t) = \frac{1}{\Gamma(\alpha)} \int_0^t f(s)(t-s)^{\alpha-1} ds, \quad -\infty \le a < t \le \infty.$$

Definition 2.3. ([21]). *A proportional-Caputo ($\mathbb{CP}$) is a hybrid operator that combines the proportional operator and the Caputo fractional derivative as:*

$$^{\mathbb{CP}}\mathfrak{D}^{\alpha}_{0,t} f(t) = \frac{1}{\Gamma(1-\alpha)} \int_0^t \Big(\mathcal{K}_1(\alpha, s) f(s) + \mathcal{K}_0(\alpha, s) f'(s)\Big)(t-s)^{-\alpha} ds$$

$$= \quad (\mathcal{K}_1(\alpha,t)f(t) + \mathcal{K}_0(\alpha,t)f'(t)) \times \frac{t^{-\alpha}}{\Gamma(1-\alpha)},$$

where $\mathcal{K}_0(\alpha,t) = \alpha C^{2\alpha} t^{1-\alpha}$ *and* $\mathcal{K}_1(\alpha,t) = (1-\alpha)t^{\alpha}$*, for* C *is constant and* $\alpha \in (0,1)$.

Moreover, as defined in the particular case where $\mathcal{K}_0$ *and* $\mathcal{K}_1$ *are depending only on* α*, the* $\mathbb{CPC}$ *operator can be defined by*

$$\begin{aligned} {}^{\mathbb{CPC}}\mathfrak{D}^{\alpha}_{0,t} f(t) &= \frac{1}{\Gamma(1-\alpha)} \int_0^t \Big(\mathcal{K}_1(\alpha) f(s) + \mathcal{K}_0(\alpha) f'(s)\Big)(t-s)^{-\alpha} ds \\ &= \mathcal{K}_1(\alpha)\, {}^{\mathbb{RL}}\mathcal{I}^{1-\alpha}_{0,t} f(t) + \mathcal{K}_0(\alpha)\, {}^{\mathbb{C}}\mathfrak{D}^{\alpha}_{0,t} f(t), \end{aligned}$$

where $\mathcal{K}_0(\alpha)$ *and* $\mathcal{K}_1(\alpha)$ *are constants with respect to* t.

Here, this study uses the specific case when $\mathcal{K}_0(\alpha) = \alpha C^{2\alpha} Q^{1-\alpha}$ and $\mathcal{K}_1(\alpha) = (1-\alpha)Q^{\alpha}$ where C and Q are constants.

Definition 2.4. ([21]). *The inverse operator of the* $\mathbb{CPC}$ *fractional derivative operator is provided by:*

$${}^{\mathbb{CPC}}\mathcal{I}^{\alpha}_{0,t} f(t) = \frac{1}{\mathcal{K}_0(\alpha)} \int_0^t (t-s)^{\alpha-1} \mathbb{E}_{1,\alpha}\left(-\frac{\mathcal{K}_1(\alpha)}{\mathcal{K}_0(\alpha)}(t-s)\right) f(s) ds,$$

which satisfies the relation below:

$${}^{\mathbb{CPC}}\mathcal{I}^{\alpha}_{0,t}\Big[{}^{\mathbb{CPC}}\mathfrak{D}^{\alpha}_{0,t} f(t)\Big] = f(t) - e^{\left(-\frac{\mathcal{K}_1(\alpha)}{\mathcal{K}_0(\alpha)} t\right)} f(0).$$

3. Formulation of the mathematical models

3.1. The integer order of the $\mathbb{MPOX}$ *model*

In this subsection, we formulate a deterministic model of the dynamics of $\mathbb{MPOX}$ transmission across two groups: humans denoted by N_h and rodents denoted by N_r. The human population has six different compartments: the susceptible (S_h), exposed (E_h), infectious (I_h), clinically ill (C_h), recovered (R_h), and vaccinated individuals (V_h). The rodent population has three compartments: the susceptible (S_r), exposed (E_r), and infectious (I_r). Thus, the total populations of humans and rodents are given by $N_h(t) = S_h(t) + E_h(t) + I_h(t) + C_h(t) + R_h(t) + V_h(t)$ and $N_r(t) = S_r(t) + E_r(t) + I_r(t)$, respectively. The transmission diagram of the population flow among these compartments is displayed in Figure 1.

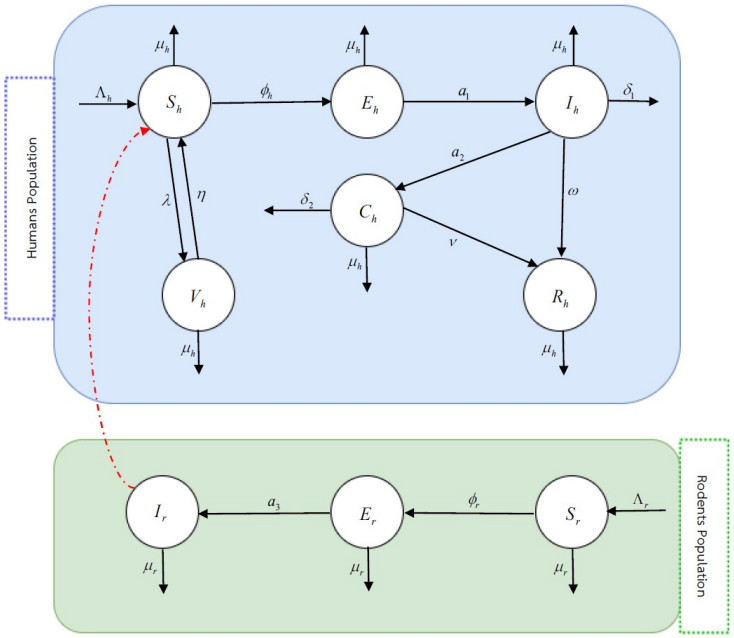

Figure 1. Transmission chart of the suggested $\mathbb{MPOX}$ model.

Here, the descriptions of the population changes of each group are presented in the following:

- **Human groups:** The amount of susceptible humans changes due to recruitment through birth rate or immigration Λ_h. The vaccinated population further increased the number in this class after the induced immunity waned at the rate η. This population class is rejected by the natural death per capital rate μ_h and by the population gaining infection after contact with infected humans or infected rodents at the rate b_1 or b_2, respectively. It is also reduced by vaccinating at the rate λ. The amount of exposed humans grows with the force of infection in the term of $\phi_h = (b_1 I_h(t) + b_2 I_r(t))/N_h(t)$ and declines by the disease progression rate a_1 and the natural death per capital rate μ_h. The amount of infected individuals increases after transitioning from the exposed class with the disease progression rate a_1. The natural recovery rate ω reduces the population in the infectious class due to immunity. This population is also reduced by the natural death rate μ_h, the disease-induced death rate δ_1, and the clinically ill rate a_2 after moving to a clinically ill class of humans. The number of clinically ill humans grows due to those who seek medical assistance after becoming sick with a clinically ill rate a_2. These individuals are decreased by disease-induced death rate δ_2 and natural death rate μ_h. Moreover, moving to the recovered class at the rate ν can reduce the population in this class. The group in the recovered compartment increases with the recovery rate of clinically ill humans ν and the natural recovery rate due to immunity ω, while it declines with the natural death rate μ_h. The susceptible individuals enter into the vaccinated class with a rate λ. The vaccinated individuals are declined by the natural death rate and the waning induced immunity with a rate η.
- **Rodent groups:** The amount of susceptible rodents changes due to recruitment through birth rate Λ_r. These individuals are decreased by interaction with infected rodents at a rate b_3 and natural death per capital rate of rodents μ_r. The amount of exposed rodents grows with the force of infection in the term $\phi_r = b_3 I_r(t)/N_r(t)$. It is declined by the natural death rate μ_r and

the progression rate a_3, which transit from exposed rodents to infected rodents. The amount of infected rodents increases from the exposed rodent's transit to infectious rodents at the rate a_3. The infected rodents are reduced due to the natural death rate μ_r.

Therefore, based on the above description, a nonlinear system of the integer-order of the $\mathbb{MPOX}$ model corresponding with nine ordinary differential equations, the so-called $\mathbb{MPOX}$ model, is shown below:

$$\begin{cases} \dfrac{dS_h(t)}{dt} = \Lambda_h - \left(\dfrac{b_1 I_h(t) + b_2 I_r(t)}{N_h(t)} + \mu_h + \lambda\right) S_h(t) + \eta V_h(t), \\ \dfrac{dE_h(t)}{dt} = \left(\dfrac{b_1 I_h(t) + b_2 I_r(t)}{N_h(t)}\right) S_h(t) - (\mu_h + a_1) E_h(t), \\ \dfrac{dI_h(t)}{dt} = a_1 E_h(t) - (\omega + a_2 + \mu_h + \delta_1) I_h(t), \\ \dfrac{dC_h(t)}{dt} = a_2 I_h(t) - (\nu + \mu_h + \delta_2) C_h(t), \\ \dfrac{dR_h(t)}{dt} = \nu C_h(t) + \omega I_h(t) - \mu_h R_h(t), \\ \dfrac{dV_h(t)}{dt} = \lambda S_h(t) - (\mu_h + \eta) V_h(t), \\ \dfrac{dS_r(t)}{dt} = \Lambda_r - \left(\dfrac{b_3 I_r(t)}{N_r(t)} + \mu_r\right) S_r(t), \\ \dfrac{dE_r(t)}{dt} = \dfrac{b_3 I_r(t) S_r(t)}{N_r(t)} - (a_3 + \mu_r) E_r(t), \\ \dfrac{dI_r(t)}{dt} = a_3 E_r(t) - \mu_r I_r(t), \end{cases} \tag{3.1}$$

where the positive initial conditions are $S_h(0) = S_{h_0}$, $E_h(0) = E_{h_0}$, $I_h(0) = I_{h_0}$, $C_h(0) = C_{h_0}$, $R_h(0) = R_{h_0}$, $V_h(0) = V_{h_0}$, $S_r(0) = S_{r_0}$, $E_r(0) = E_{r_0}$, and $I_r(0) = I_{r_0}$. The details of each all positive parameter are included and displayed in Table 1.

Table 1. The details of dependent parameters of the $\mathbb{MPOX}$ model (3.1).

Parameters	Description
Λ_h, Λ_r	The recruitment rate for susceptible humans and rodents, respectively.
b_1, b_2, b_2	Contact rate between infected humans and susceptible humans, rodents and susceptible humans, and rodents and susceptible rodents, respectively.
a_1	Disease progression rate from exposed humans to infected humans.
a_2	Clinically ill rate.
a_3	Progression rate from exposed rodents to infected rodents.
ω	Natural recovery rate due to immunity.
ν	The rate of recovery for clinically ill humans.
η	Waning induced immunity.
λ	Vaccinated against monkeypox.
δ_1, δ_2	Disease-induced death rate for infectious and clinically ill humans, respectively.
μ_h, μ_r	Natural death per capital rate of humans and rodents, respectively.

3.2. The $\mathbb{MPOX}$ model under the $\mathbb{CPC}$ derivative operator

As we know, fractional infectious models have specific hereditary properties and describe memory regarding disease dynamics because they employ fractional derivatives with a higher degree of freedom to account for more complex diseases and provide knowledge into the behavior and control of epidemic diseases. Consequently, this subsection further develops the integer order $\mathbb{MPOX}$ model (3.1) utilizing the $\mathbb{CPC}$ derivative operator as follows:

$$\begin{cases} {}^{\mathbb{CPC}}\mathfrak{D}^{\alpha}_{0,t}S_h(t) = \mathbb{F}_1(t, S_h(t), E_h(t), I_h(t), C_h(t), R_h(t), V_h(t), S_r(t), E_r(t), I_r(t)), \\ {}^{\mathbb{CPC}}\mathfrak{D}^{\alpha}_{0,t}E_h(t) = \mathbb{F}_2(t, S_h(t), E_h(t), I_h(t), C_h(t), R_h(t), V_h(t), S_r(t), E_r(t), I_r(t)), \\ {}^{\mathbb{CPC}}\mathfrak{D}^{\alpha}_{0,t}I_h(t) = \mathbb{F}_3(t, S_h(t), E_h(t), I_h(t), C_h(t), R_h(t), V_h(t), S_r(t), E_r(t), I_r(t)), \\ {}^{\mathbb{CPC}}\mathfrak{D}^{\alpha}_{0,t}C_h(t) = \mathbb{F}_4(t, S_h(t), E_h(t), I_h(t), C_h(t), R_h(t), V_h(t), S_r(t), E_r(t), I_r(t)), \\ {}^{\mathbb{CPC}}\mathfrak{D}^{\alpha}_{0,t}R_h(t) = \mathbb{F}_5(t, S_h(t), E_h(t), I_h(t), C_h(t), R_h(t), V_h(t), S_r(t), E_r(t), I_r(t)), \\ {}^{\mathbb{CPC}}\mathfrak{D}^{\alpha}_{0,t}V_h(t) = \mathbb{F}_6(t, S_h(t), E_h(t), I_h(t), C_h(t), R_h(t), V_h(t), S_r(t), E_r(t), I_r(t)), \\ {}^{\mathbb{CPC}}\mathfrak{D}^{\alpha}_{0,t}S_r(t) = \mathbb{F}_7(t, S_h(t), E_h(t), I_h(t), C_h(t), R_h(t), V_h(t), S_r(t), E_r(t), I_r(t)), \\ {}^{\mathbb{CPC}}\mathfrak{D}^{\alpha}_{0,t}E_r(t) = \mathbb{F}_8(t, S_h(t), E_h(t), I_h(t), C_h(t), R_h(t), V_h(t), S_r(t), E_r(t), I_r(t)), \\ {}^{\mathbb{CPC}}\mathfrak{D}^{\alpha}_{0,t}I_r(t) = \mathbb{F}_9(t, S_h(t), E_h(t), I_h(t), C_h(t), R_h(t), V_h(t), S_r(t), E_r(t), I_r(t)), \end{cases} \tag{3.2}$$

where $\mathbb{F}_j = \mathbb{F}_j(t, S_h(t), E_h(t), I_h(t), C_h(t), R_h(t), V_h(t), S_r(t), E_r(t), I_r(t))$, for $j = 1, 2, \ldots, 9$ and $\mathbb{F}_j$ for the suggested model are given by

$$\begin{cases} \mathbb{F}_1(t, S_h(t)) = \Lambda_h - (\phi_h + c_1)S_h(t) + \eta V_h(t), \\ \mathbb{F}_2(t, E_h(t)) = \phi_h S_h(t) - c_2 E_h(t), \\ \mathbb{F}_3(t, I_h(t)) = a_1 E_h(t) - c_3 I_h(t), \\ \mathbb{F}_4(t, C_h(t)) = a_2 I_h(t) - c_4 C_h(t), \\ \mathbb{F}_5(t, R_h(t)) = \nu C_h(t) + \omega I_h(t) - \mu_h R_h(t), \\ \mathbb{F}_6(t, V_h(t)) = \lambda S_h(t) - c_5 V_h(t), \\ \mathbb{F}_7(t, S_r(t)) = \Lambda_r - \phi_r S_r(t) - \mu_r S_r(t), \\ \mathbb{F}_8(t, E_r(t)) = \phi_r S_r(t) - c_6 E_r(t), \\ \mathbb{F}_9(t, I_r(t)) = a_3 E_r(t) - \mu_r I_r(t), \end{cases} \tag{3.3}$$

with $\phi_h = (b_1 I_h(t) + b_2 I_r(t))/N_h(t)$, $\phi_r = b_3 I_r(t)/N_r(t)$, $c_1 = \mu_h + \lambda$, $c_2 = \mu_h + a_1$, $c_3 = \omega + a_2 + \mu_h + \delta_1$, $c_4 = \nu + \mu_h + \delta_2$, $c_5 = \mu_h + \eta$, and $c_6 = a_3 + \mu_r$ with $S_{h_0} \geq 0$, $E_{h_0} \geq 0$, $I_{h_0} \geq 0$, $C_{h_0} \geq 0$, $R_{h_0} \geq 0$, $V_{h_0} \geq 0$, $S_{r_0} \geq 0$, $E_{r_0} \geq 0$, and $I_{r_0} \geq 0$. The suggested model (3.2) is said to be the $\mathbb{CPC}$-$\mathbb{MPOX}$ model.

4. Model analysis

4.1. Positiveness and boundedness

Since the variables in real-world phenomena have positive values, particularly the epidemic model based on the human population, all variables and parameters are considered to be positive. Moreover, the invariant region is essential in mathematical modeling as it guarantees that solutions remain biologically feasible and mathematically meaningful. In this part, we investigate the factors that guarantee the solutions of the $\mathbb{CPC}$-$\mathbb{MPOX}$ model (3.2) are positive, and we locate the invariant area,

ensuring that the solution is bounded. To achieve this purpose, we define

$$\mathbb{R}^9_+ = \left\{\mathbb{F} \in \mathbb{R}^9 : \mathbb{F} \geq 0 \text{ and } \mathbb{F}(t) = (S_h(t), E_h(t), I_h(t), C_h(t), R_h(t), V_h(t), S_r(t), E_r(t), I_r(t))^T\right\}.$$

Theorem 4.1. *All solutions of the* $\mathbb{CPC}$-$\mathbb{MPOX}$ *model* (3.2) *under the initial conditions are bounded in* $\mathbb{R}^9_+$.

Proof. From the $\mathbb{CPC}$-$\mathbb{MPOX}$ model (3.2), we obtain

$$\begin{cases} {}^{\mathbb{CPC}}\mathfrak{D}^{\alpha}_{0,t} S_h(t) = \Lambda_h + \eta V_h(t) \geq 0, \\ {}^{\mathbb{CPC}}\mathfrak{D}^{\alpha}_{0,t} E_h(t) = \phi_h S_h(t) \geq 0, \\ {}^{\mathbb{CPC}}\mathfrak{D}^{\alpha}_{0,t} I_h(t) = a_1 E_h(t) \geq 0, \\ {}^{\mathbb{CPC}}\mathfrak{D}^{\alpha}_{0,t} C_h(t) = a_2 I_h(t) \geq 0, \\ {}^{\mathbb{CPC}}\mathfrak{D}^{\alpha}_{0,t} R_h(t) = \nu C_h(t) + \omega I_h(t) \geq 0, \\ {}^{\mathbb{CPC}}\mathfrak{D}^{\alpha}_{0,t} V_h(t) = \lambda S_h(t) \geq 0, \\ {}^{\mathbb{CPC}}\mathfrak{D}^{\alpha}_{0,t} S_r(t) = \Lambda_r \geq 0, \\ {}^{\mathbb{CPC}}\mathfrak{D}^{\alpha}_{0,t} E_r(t) = \phi_r S_r(t) \geq 0, \\ {}^{\mathbb{CPC}}\mathfrak{D}^{\alpha}_{0,t} I_r(t) = a_3 E_r(t) \geq 0. \end{cases} \tag{4.1}$$

If a set of the conditions $(S_{h_0}, E_{h_0}, I_{h_0}, C_{h_0}, R_{h_0}, V_{h_0}, S_{r_0}, E_{r_0}, I_{r_0}) \in \mathbb{R}^9_+$, then according to the above system (4.1), the solution $\mathbb{F}$ cannot avoid from the hyper-planes: (S_h, E_h, I_h, C_h, R_h, V_h, S_r, E_r, I_r) = (0, 0, 0, 0, 0, 0, 0, 0, 0). Additionally, the vector field points into $\mathbb{R}^9_+$ on each hyperplane that is surrounded by the nonnegative constants. This means that $\mathbb{R}^9_+$ is the positively invariant region. □

Theorem 4.2. *Let a positive set of solutions* $(S_h(t), E_h(t), I_h(t), C_h(t), R_h(t), V_h(t), S_r(t), E_r(t), I_r(t))$ *under the initial conditions. Then, there exists a domain* $\Omega = \Omega_h \times \Omega_r \subset \mathbb{R}^6_+ \times \mathbb{R}^3_+$, *that is positively invariant so that*

$$\Omega_h = \left\{(S_h(t), E_h(t), I_h(t), C_h(t), R_h(t), V_h(t)) \in \mathbb{R}^6_+ \quad \text{and} \quad N_h \leq \Lambda_h/\mu_h\right\}, \tag{4.2}$$

$$\Omega_r = \left\{(S_r(t), E_r(t), I_r(t)) \in \mathbb{R}^3_+ \quad \text{and} \quad N_h \leq \Lambda_r/\mu_r\right\}. \tag{4.3}$$

Proof. Since $N_h(t) = S_h(t) + E_h(t) + I_h(t) + C_h(t) + R_h(t) + V_h(t)$, then from the proposed model (3.2), we have

$$\begin{aligned} {}^{\mathbb{CPC}}\mathfrak{D}^{\alpha}_{0,t} N_h(t) &= {}^{\mathbb{CPC}}\mathfrak{D}^{\alpha}_{0,t} S_h(t) + {}^{\mathbb{CPC}}\mathfrak{D}^{\alpha}_{0,t} E_h(t) + {}^{\mathbb{CPC}}\mathfrak{D}^{\alpha}_{0,t} I_h(t) \\ &\quad + {}^{\mathbb{CPC}}\mathfrak{D}^{\alpha}_{0,t} C_h(t) + {}^{\mathbb{CPC}}\mathfrak{D}^{\alpha}_{0,t} R_h(t) + {}^{\mathbb{CPC}}\mathfrak{D}^{\alpha}_{0,t} V_h(t) \\ &= \Lambda_h - \mu_h N_h(t) - \delta_1 I_h(t) - \delta_2 C_h(t). \end{aligned}$$

In the case of no disease, we get ${}^{\mathbb{CPC}}\mathfrak{D}^{\alpha}_{0,t} N_h(t) = \Lambda_h - \mu_h N_h(t)$. It implies that

$${}^{\mathbb{CPC}}\mathfrak{D}^{\alpha}_{0,t} N_h(t) \leq 0 \quad \text{if} \quad N_h(t) \geq \frac{\Lambda_h}{\mu_h}, \quad \text{for all} \quad t \in [0, T].$$

By a particular comparison principle, we obtain

$$N_h(t) \leq N_h(0)e^{-\mu_h t} + \frac{\Lambda_h}{\mu_h}(1 - e^{-\mu_h t}).$$

Then, we get

$$N_h(t) \leq \frac{\Lambda_h}{\mu_h} \quad \text{if} \quad N_h(0) \leq \frac{\Lambda_h}{\mu_h}.$$

Thus, the feasible region of human groups (4.2) is completed.

Similarly, since $N_r(t) = S_r(t) + E_r(t) + I_r(t)$, then

$${}^{\mathbb{CPC}}\mathfrak{D}^{\alpha}_{0,t} N_r(t) = {}^{\mathbb{CPC}}\mathfrak{D}^{\alpha}_{0,t} S_r(t) + {}^{\mathbb{CPC}}\mathfrak{D}^{\alpha}_{0,t} E_r(t) + {}^{\mathbb{CPC}}\mathfrak{D}^{\alpha}_{0,t} I_r(t) = \Lambda_r - \mu_r N_r(t).$$

It implies that

$${}^{\mathbb{CPC}}\mathfrak{D}^{\alpha}_{0,t} N_r(t) \leq 0 \quad \text{if} \quad N_r(t) \geq \frac{\Lambda_r}{\mu_r}, \quad \text{for all} \quad t \in [0, T].$$

By a particular comparison principle, we have

$$N_r(t) \leq N_r(0)e^{-\mu_r t} + \frac{\Lambda_r}{\mu_r}(1 - e^{-\mu_r t}).$$

Then, we have

$$N_r(t) \leq \frac{\Lambda_r}{\mu_r} \quad \text{if} \quad N_r(0) \leq \frac{\Lambda_r}{\mu_r}.$$

Thus, the feasible region of rodent groups (4.3) is obtained. This shows the boundedness of the solutions for the $\mathbb{CPC}$-$\mathbb{MPOX}$ model (3.2). Hence, the region $\Omega = \Omega_h \times \Omega_r$, defined as (4.2) and (4.3), is positively invariant. We therefore conclude that the proposed model is epidemiologically feasible and well-posed in Ω. The proof is complete. □

4.2. The stability of the equilibria

The equilibrium points of the the $\mathbb{CPC}$-$\mathbb{MPOX}$ model (3.2) can be calculated by setting the right-hand side equal to zero. This gives two possible positive equilibria, which are

- The $\mathbb{MPOX}$ free equilibrium ($\mathfrak{E}^0_{MFE}$); this point is defined when there is no disease in the population:

$$\mathfrak{E}^0_{MFE} = (S^0_h, E^0_h, I^0_h, C^0_h, R^0_h, V^0_h, S^0_r, E^0_r, I^0_r) = \left(\frac{c_5\Lambda_h}{c_1c_5 - \lambda\eta}, 0, 0, 0, 0, \frac{\lambda\Lambda_h}{c_1c_5 - \lambda\eta}, \frac{\Lambda_r}{\mu_r}, 0, 0\right).$$

  Note that: $c_1c_5 - \lambda\eta = \mu_h(\mu_h + \eta + \lambda) > 0$, $N^0_h = S^0_h + E^0_h + I^0_h + C^0_h + R^0_h + V^0_h$, and $N^0_r = S^0_r + E^0_r + I^0_r$.
- The $\mathbb{MPOX}$ endemic equilibrium ($\mathfrak{E}^*_{MEE}$); this point is defined when there is disease transmission in the population:

$$\mathfrak{E}^*_{MEE} = (S^*_h, E^*_h, I^*_h, C^*_h, R^*_h, V^*_h, S^*_r, E^*_r, I^*_r),$$

  where

$$\begin{aligned}
S^*_h &= \frac{c_5\Lambda_h}{c_5(\phi_h + c_1) - \eta\lambda}, \quad E^*_h = \frac{c_5\Lambda_h\phi_h}{c_2[c_5(\phi_h + c_1) - \eta\lambda]}, \quad I^*_h = \frac{c_5\Lambda_h a_1\phi_h}{c_2c_3[c_5(\phi_h + c_1) - \eta\lambda]},\\
C^*_h &= \frac{c_5\Lambda_h a_1a_2\phi_h}{c_2c_3c_4[c_5(\phi_h + c_1) - \eta\lambda]},\\
R^*_h &= \frac{\nu c_5\Lambda_h a_1a_2\phi_h}{\mu_h c_2c_3c_4[c_5(\phi_h + c_1) - \eta\lambda]} + \frac{\omega c_5\Lambda_h a_1\phi_h}{\mu_h c_2c_3[c_5(\phi_h + c_1) - \eta\lambda]},\\
V^*_h &= \frac{c_5\Lambda_h\lambda}{c_5[c_5(\phi_h + c_1) - \eta\lambda]}, \quad S^*_r = \frac{\Lambda_r}{\phi_r + \mu_r}, \quad E^*_r = \frac{\phi_r\Lambda_r}{c_6(\phi_r + \mu_r)}, \quad I^*_r = \frac{a_3\phi_r\Lambda_r}{c_6\mu_r(\phi_r + \mu_r)}.
\end{aligned}$$

Next, the basic reproduction number is conducted as an epidemic indicator. It is an essential fundamental epidemiological parameter used to assess the long-term dynamics of the epidemic, which is denoted by $\Re_0$. It is also defined as the expected number of secondary infections generated by a single infected individual throughout their infectious period. The basic reproduction number can be used as a disease control measure because it indicates the spread of a disease in terms of transmission within a population. It helps determine whether an outbreak or epidemic will occur or the infection will eventually disappear. Here, we will calculate it by using the next-generation technique as in [53]. For the proposed model, the disease-free state variables are S_h, R_h, S_r while the infected state variables are $E_h, I_h, C_h, V_h, E_r, I_r$. Therefore,

$$\mathcal{F} = \begin{pmatrix} 0 & \frac{b_1 S_h^0}{N_h^0} & 0 & 0 & 0 & \frac{b_2 S_h^0}{N_h^0} \\ 0 & 0 & 0 & 0 & 0 & 0 \\ 0 & 0 & 0 & 0 & 0 & 0 \\ 0 & 0 & 0 & 0 & 0 & 0 \\ 0 & 0 & 0 & 0 & 0 & b_3 \\ 0 & 0 & 0 & 0 & 0 & 0 \end{pmatrix} \quad \text{and} \quad \mathcal{V} = \begin{pmatrix} c_2 & 0 & 0 & 0 & 0 & 0 \\ -a_1 & c_3 & 0 & 0 & 0 & 0 \\ 0 & -a_2 & c_4 & 0 & 0 & 0 \\ 0 & 0 & 0 & c_5 & 0 & 0 \\ 0 & 0 & 0 & 0 & c_6 & 0 \\ 0 & 0 & 0 & 0 & -a_3 & \mu_r \end{pmatrix},$$

where $\mathcal{F}$ and $\mathcal{V}$ denote the transmission and transitions matrices, respectively. Then, the next-generation matrix is provided as below:

$$\mathcal{F}\mathcal{V}^{-1} = \begin{pmatrix} \frac{a_1 b_1 S_h^0}{c_2 c_3 N_h^0} & \frac{b_1 S_h^0}{c_3 N_h^0} & 0 & 0 & \frac{a_3 b_2 S_h^0}{c_6 \mu_r N_h^0} & \frac{b_2 S_h^0}{\mu_r N_h^0} \\ 0 & 0 & 0 & 0 & 0 & 0 \\ 0 & 0 & 0 & 0 & 0 & 0 \\ 0 & 0 & 0 & 0 & 0 & 0 \\ 0 & 0 & 0 & 0 & \frac{a_3 b_3}{c_6 \mu_r} & \frac{b_3}{\mu_r} \\ 0 & 0 & 0 & 0 & 0 & 0 \end{pmatrix}.$$

This implies the spectral radius of (4.2) ($\Re_0$)

$$\Re_0 = \max\{\Re_0^h, \Re_0^r\} = \max\left\{\frac{a_1 b_1 S_h^0}{c_2 c_3 N_h^0}, \frac{a_3 b_3}{c_6 \mu_r}\right\}.$$

Remark 4.3. *We can notice that:*

- *If* $\Re_h^0 > 1$ *and* $\Re_r^0 > 1$, *then* $\Re_0 > 1$.
- *If* $\Re_h^0 < 1$ *and* $\Re_r^0 > 1$, *then* $\Re_0 = \Re_r^0 > 1$.
- *If* $\Re_h^0 > 1$ *and* $\Re_r^0 < 1$, *then* $\Re_0 = \Re_h^0 > 1$.
- *If* $\Re_h^0 < 1$ *and* $\Re_r^0 < 1$, *then* $\Re_0 < 1$.

For the following two theorems, the stability of the equilibrium points will be analyzed. To do this, the Jacobian matrix ($\mathcal{J}$) of the system is given by

$$\mathcal{J} = \begin{pmatrix} -\frac{b_1 I_h + b_2 I_r}{N_h} - c_1 & 0 & -\frac{b_1 S_h}{N_h} & 0 & 0 & \eta & 0 & 0 & -\frac{b_2 S_h}{N_h} \\ \frac{b_1 I_h + b_2 I_r}{N_h} & -c_2 & \frac{b_1 S_h}{N_h} & 0 & 0 & 0 & 0 & 0 & \frac{b_2 S_h}{N_h} \\ 0 & a_1 & -c_3 & 0 & 0 & 0 & 0 & 0 & 0 \\ 0 & 0 & a_2 & -c_4 & 0 & 0 & 0 & 0 & 0 \\ 0 & 0 & \omega & \nu & -\mu_h & 0 & 0 & 0 & 0 \\ \lambda & 0 & 0 & 0 & 0 & -c_5 & 0 & 0 & 0 \\ 0 & 0 & 0 & 0 & 0 & 0 & -\frac{b_3 I_r}{N_r} - \mu_r & 0 & -\frac{b_3 S_r}{N_r} \\ 0 & 0 & 0 & 0 & 0 & 0 & \frac{b_3 I_r}{N_r} & -c_6 & \frac{b_3 S_r}{N_r} \\ 0 & 0 & 0 & 0 & 0 & 0 & 0 & a_3 & -\mu_r \end{pmatrix}. \tag{4.4}$$

Theorem 4.4. *If $\Re_0 < 1$, then the $\mathbb{MPOX}$ free equilibrium of the $\mathbb{CPC}$-$\mathbb{MPOX}$ model* (3.2) *is locally asymptotically stable with the necessary and sufficient criteria:*

$$|arg(\theta_i)| > \frac{\alpha\pi}{2}, \quad i = 1, 2, ..., 9. \tag{4.5}$$

Proof. From the asumption $\Re_0 < 1$, it implies that $\Re_0^h < 1$ and $\Re_0^r < 1$. By applying matrix (4.4) at the point $\mathfrak{E}_{MFE}^0$, we have

$$\mathcal{J}(\mathfrak{E}_{MFE}^0) = \begin{pmatrix} -c_1 & 0 & -\frac{b_1 S_h^0}{N_h^0} & 0 & 0 & \eta & 0 & 0 & -\frac{b_2 S_h^0}{N_h^0} \\ 0 & -c_2 & \frac{b_1 S_h^0}{N_h^0} & 0 & 0 & 0 & 0 & 0 & \frac{b_2 S_h^0}{N_h^0} \\ 0 & a_1 & -c_3 & 0 & 0 & 0 & 0 & 0 & 0 \\ 0 & 0 & a_2 & -c_4 & 0 & 0 & 0 & 0 & 0 \\ 0 & 0 & \omega & \nu & -\mu_h & 0 & 0 & 0 & 0 \\ \lambda & 0 & 0 & 0 & 0 & -c_5 & 0 & 0 & 0 \\ 0 & 0 & 0 & 0 & 0 & 0 & -\mu_r & 0 & -b_3 \\ 0 & 0 & 0 & 0 & 0 & 0 & 0 & -c_6 & b_3 \\ 0 & 0 & 0 & 0 & 0 & 0 & 0 & a_3 & -\mu_r \end{pmatrix}.$$

Then, the characteristic equation is computed by $|\mathcal{J}(\mathfrak{E}_{MFE}^0) - \theta\hat{I}| = 0$, and $\hat{I}$ is a identity matrix. This yields the eigenvalues as the following:

$$\begin{aligned} \theta_1 &= -c_4, \qquad \theta_2 = -\mu_r, \qquad \theta_3 = -\mu_h, \\ \theta_{4,5} &= \frac{1}{2}\left(-(c_1 + c_5) \pm \sqrt{(c_1 + c_5)^2 - 4(\mu_h(\mu_h + \eta + \lambda))}\right), \\ \theta_{6,7} &= \frac{1}{2}\left(-(c_2 + c_3) \pm \sqrt{(c_2 + c_3)^2 - 4\left(c_2 c_3 - \frac{a_1 b_1 S_h^0}{N_h^0}\right)}\right), \\ \theta_{8,9} &= \frac{1}{2}\left(-(\mu_r + c_6) \pm \sqrt{(\mu_r + c_6)^2 - 4(\mu_r c_6 - a_3 b_3)}\right). \end{aligned}$$

Obviously, the eigenvalues $\theta_1, \theta_2, \theta_3$, and $\theta_{4,5}$ have negative real parts. Since $\Re_0^h < 1$ and $\Re_0^r < 1$, then the eigenvalues $\theta_{6,7}$ and $\theta_{8,9}$ also have negative real parts, respectively. This assures the assumption (4.5) with $0 < \alpha \leq 1$. Therefore, the point $\mathfrak{E}_{MFE}^0$ is locally asymptotically stable. □

For the following theorem, we will utilize the Routh-Hurwitz criterion to investigate the local stability of endemic equilibria. Here, we will determine the conditions under which the endemic equilibrium point is locally asymptotically stable. The Jacobian matrix (4.4) yields the following matrix for $\mathfrak{E}^*_{MEE}$:

$$\mathcal{J}_1(\mathfrak{E}^*_{MEE}) = \begin{pmatrix} -\frac{b_1 I_h^* + b_2 I_r^*}{N_h^*} - c_1 & 0 & -\frac{b_1 S_h^*}{N_h^*} & 0 & 0 & \eta & 0 & 0 & -\frac{b_2 S_h^*}{N_h^*} \\ \frac{b_1 I_h^* + b_2 I_r^*}{N_h^*} & -c_2 & \frac{b_1 S_h^*}{N_h^*} & 0 & 0 & 0 & 0 & 0 & \frac{b_2 S_h^*}{N_h^*} \\ 0 & a_1 & -c_3 & 0 & 0 & 0 & 0 & 0 & 0 \\ 0 & 0 & a_2 & -c_4 & 0 & 0 & 0 & 0 & 0 \\ 0 & 0 & \omega & \nu & -\mu_h & 0 & 0 & 0 & 0 \\ \lambda & 0 & 0 & 0 & 0 & -c_5 & 0 & 0 & 0 \\ 0 & 0 & 0 & 0 & 0 & 0 & -\frac{b_3 I_r^*}{N_r^*} - \mu_r & 0 & -\frac{b_3 S_r^*}{N_r^*} \\ 0 & 0 & 0 & 0 & 0 & 0 & \frac{b_3 I_r^*}{N_r^*} & -c_6 & \frac{b_3 S_r^*}{N_r^*} \\ 0 & 0 & 0 & 0 & 0 & 0 & 0 & a_3 & -\mu_r \end{pmatrix}.$$

We can easily see two negative eigenvalues; one is $\omega_1 = -\mu_h$, and another one is $\omega_2 = -c_4$. For the rest of the equilibrium points, we consider the reduced matrix

$$\mathcal{J}_2(\mathfrak{E}^*_{MEE}) = \begin{pmatrix} -\frac{b_1 I_h^* + b_2 I_r^*}{N_h^*} - c_1 & 0 & -\frac{b_1 S_h^*}{N_h^*} & \eta & 0 & 0 & -\frac{b_2 S_h^*}{N_h^*} \\ \frac{b_1 I_h^* + b_2 I_r^*}{N_h^*} & -c_2 & \frac{b_1 S_h^*}{N_h^*} & 0 & 0 & 0 & \frac{b_2 S_h^*}{N_h^*} \\ 0 & a_1 & -c_3 & 0 & 0 & 0 & 0 \\ \lambda & 0 & 0 & -c_5 & 0 & 0 & 0 \\ 0 & 0 & 0 & 0 & -\frac{b_3 I_r^*}{N_r^*} - \mu_r & 0 & -\frac{b_3 S_r^*}{N_r^*} \\ 0 & 0 & 0 & 0 & \frac{b_3 I_r^*}{N_r^*} & -c_6 & \frac{b_3 S_r^*}{N_r^*} \\ 0 & 0 & 0 & 0 & 0 & a_3 & -\mu_r \end{pmatrix}.$$

This yields the associated characteristic equation as follows:

$$\omega^7 + \epsilon_1\omega^6 + \epsilon_2\omega^5 + \epsilon_3\omega^4 + \epsilon_4\omega^3 + \epsilon_5\omega^2 + \epsilon_6\omega + \epsilon_7 = 0, \tag{4.6}$$

with ϵ_k denoting the coefficients of $\omega^{7-k}, k = 1, 2, 3, \ldots, 7$ after resetting the polynomial equation in the formula form. Since the proof of the local asymptotic stable needs the negative real parts of all roots of (4.6), we use the Routh-Hurwitz criteria to obtain the conditions for the stability of $\mathfrak{E}^*_{MEE}$. We define the following notation, $h_1 = (\epsilon_1\epsilon_2 - \epsilon_3)/\epsilon_1$, $h_2 = (\epsilon_1\epsilon_4 - \epsilon_5)/\epsilon_1$, $h_3 = (\epsilon_1\epsilon_6 - \epsilon_7)/\epsilon_1$, $g_1 = (\epsilon_3 h_1 - \epsilon_1 h_2)/h_1$, $g_2 = (\epsilon_5 h_1 - \epsilon_1 h_3)/h_1$, $g_3 = \epsilon_7$, $d_1 = (h_2 g_1 - h_1 g_2)/g_1$, $d_2 = (h_3 g_1 - h_1 g_3)/g_1$, $e_1 = (g_2 d_1 - g_1 d_2)/d_1$, $e_2 = g_3$, and $f_1 = (d_2 e_1 - d_1 e_2)/e_1$.

Thus, the Hurwitz assumptions concerning (4.6), which ensure that all roots have negative real parts, are as follows: $(\mathcal{H}_1)$. (i) $\epsilon_1 > 0$; (ii) $\epsilon_7 > 0$; (iii) $\epsilon_1\epsilon_2 > \epsilon_3$; (iv) $\epsilon_1\epsilon_2\epsilon_3 + \epsilon_1\epsilon_5 > \epsilon_1^2\epsilon_4 + \epsilon_3^2$; (v) $h_2 g_1 > h_1 g_2$; (vi) $g_2 d_1 > g_1 d_2$; and (vii) $d_2 e_1 > d_1 e_2$. Therefore, we can conclude this part by the following theorem:

Theorem 4.5. *Suppose that the necessary and sufficient assumption $(\mathcal{H}_1)$ of Hurwitz criteria is satisfied, then the $\mathbb{MPOX}$ endemic equilibrium of the $\mathbb{CPC}$-$\mathbb{MPOX}$ model* (3.2) *is locally asymptotically stable.*

5. Qualitative analysis

In this part, an analysis of the $\mathbb{CPC}$-$\mathbb{MPOX}$ model (3.2) will be investigated applying Banach's contraction mapping principle [54]. First, the Banach space on $[0, T]$ for all continuous real-valued functions is given by $\mathbb{X} = C(\mathcal{I} \times \mathbb{R}^9, \mathbb{R})$ under the norm $\|\mathcal{Y}\| = \|(S_h, E_h, I_h, C_h, R_h, V_h, S_r, E_r, I_r)\| = \|S_h\| + \|E_h\| + \|I_h\| + \|C_h\| + \|R_h\| + \|V_h\| + \|S_r\| + \|E_r\| + \|I_r\|$, where S_h, E_h, I_h, C_h, R_h, V_h, S_r, E_r, $I_r \in \mathbb{X}$ and $\|S_h\| = \sup_{t\in[0,T]} |S_h(t)| = \mathfrak{B}_{h_1}$, $\|E_h\| = \sup_{t\in[0,T]} |E_h(t)| = \mathfrak{B}_{h_2}$, $\|I_h\| = \sup_{t\in[0,T]} |I_h(t)| = \mathfrak{B}_{h_3}$, $\|C_h\| = \sup_{t\in[0,T]} |C_h(t)| = \mathfrak{B}_{h_4}$, $\|R_h\| = \sup_{t\in[0,T]} |R_h(t)| = \mathfrak{B}_{h_5}$, $\|V_h\| = \sup_{t\in[0,T]} |V_h(t)| = \mathfrak{B}_{h_6}$, $\|S_r\| = \sup_{t\in[0,T]} |S_r(t)| = \mathfrak{B}_{r_1}$, $\|E_r\| = \sup_{t\in[0,T]} |E_r(t)| = \mathfrak{B}_{r_2}$, and $\|I_r\| = \sup_{t\in[0,T]} |I_r(t)| = \mathfrak{B}_{r_3}$. Next, assume $\mathbb{F} \in \mathbb{X}$ and $\mathcal{Y} \in C([0, T], \mathbb{R})$, and the $\mathbb{CPC}$-$\mathbb{MPOX}$ model (3.2) can be presented as

$$\begin{cases} {}^{\mathbb{CPC}}\mathfrak{D}^{\alpha}_{0,t}\mathcal{Y}(t) = \mathbb{F}(t, \mathcal{Y}(t)), \quad t \in [0, T], \quad \alpha \in (0, 1], \\ \mathcal{Y}(0) = \mathcal{Y}_0, \end{cases} \tag{5.1}$$

where

$$\mathcal{Y}(t) = \begin{pmatrix} S_h(t) \\ E_h(t) \\ I_h(t) \\ C_h(t) \\ R_h(t) \\ V_h(t) \\ S_r(t) \\ E_r(t) \\ I_r(t) \end{pmatrix}, \quad \mathcal{Y}(0) = \begin{pmatrix} S_h(0) \\ E_h(0) \\ I_h(0) \\ C_h(0) \\ R_h(0) \\ V_h(0) \\ S_r(0) \\ E_r(0) \\ I_r(0) \end{pmatrix} = \begin{pmatrix} S_{h_0} \\ E_{h_0} \\ I_{h_0} \\ C_{h_0} \\ R_{h_0} \\ V_{h_0} \\ S_{r_0} \\ E_{r_0} \\ I_{r_0} \end{pmatrix}, \quad \mathbb{F}(t, \mathcal{Y}(t)) = \begin{pmatrix} \mathbb{F}_1(t, S_h) \\ \mathbb{F}_2(t, E_h) \\ \mathbb{F}_3(t, I_h) \\ \mathbb{F}_4(t, C_h) \\ \mathbb{F}_5(t, R_h) \\ \mathbb{F}_6(t, V_h) \\ \mathbb{F}_7(t, S_r) \\ \mathbb{F}_8(t, E_r) \\ \mathbb{F}_9(t, I_r) \end{pmatrix},$$

when $\mathbb{G}_i$, $i = 1, 2, \ldots, 9$ are given by (3.3). Then, the problem (5.1) can be written applying Definition 2.4 as below

$$\mathcal{Y}(t) - e^{\left(-\frac{K_1(\alpha)}{K_0(\alpha)}t\right)}\mathcal{Y}(0) = \frac{1}{K_0(\alpha)} \int_0^t (t-s)^{\alpha-1} \mathbb{E}_{1,\alpha}\left(-\frac{K_1(\alpha)}{K_0(\alpha)}(t-s)\right) \mathbb{F}(s, \mathcal{Y}(s))ds. \tag{5.2}$$

From the problem (5.1), the Eq (5.2) can be presented in the integral form:

$$S_h(t) = e^{\left(-\frac{K_1(\alpha)}{K_0(\alpha)}t\right)}S_{h_0} + \frac{1}{K_0(\alpha)} \int_0^t (t-s)^{\alpha-1} \mathbb{E}_{1,\alpha}\left(-\frac{K_1(\alpha)}{K_0(\alpha)}(t-s)\right) \mathbb{F}_1(s, S_h(s))ds, \tag{5.3}$$

$$E_h(t) = e^{\left(-\frac{K_1(\alpha)}{K_0(\alpha)}t\right)}E_{h_0} + \frac{1}{K_0(\alpha)} \int_0^t (t-s)^{\alpha-1} \mathbb{E}_{1,\alpha}\left(-\frac{K_1(\alpha)}{K_0(\alpha)}(t-s)\right) \mathbb{F}_2(s, E_h(s))ds, \tag{5.4}$$

$$I_h(t) = e^{\left(-\frac{K_1(\alpha)}{K_0(\alpha)}t\right)}I_{h_0} + \frac{1}{K_0(\alpha)} \int_0^t (t-s)^{\alpha-1} \mathbb{E}_{1,\alpha}\left(-\frac{K_1(\alpha)}{K_0(\alpha)}(t-s)\right) \mathbb{F}_3(s, I_h(s))ds, \tag{5.5}$$

$$C_h(t) = e^{\left(-\frac{K_1(\alpha)}{K_0(\alpha)}t\right)}C_{h_0} + \frac{1}{K_0(\alpha)} \int_0^t (t-s)^{\alpha-1} \mathbb{E}_{1,\alpha}\left(-\frac{K_1(\alpha)}{K_0(\alpha)}(t-s)\right) \mathbb{F}_4(s, C_h(s))ds, \tag{5.6}$$

$$R_h(t) = e^{\left(-\frac{K_1(\alpha)}{K_0(\alpha)}t\right)}R_{h_0} + \frac{1}{K_0(\alpha)} \int_0^t (t-s)^{\alpha-1} \mathbb{E}_{1,\alpha}\left(-\frac{K_1(\alpha)}{K_0(\alpha)}(t-s)\right) \mathbb{F}_5(s, R_h(s))ds, \tag{5.7}$$

$$V_h(t) = e^{\left(-\frac{K_1(\alpha)}{K_0(\alpha)}t\right)}V_{h_0} + \frac{1}{K_0(\alpha)} \int_0^t (t-s)^{\alpha-1} \mathbb{E}_{1,\alpha}\left(-\frac{K_1(\alpha)}{K_0(\alpha)}(t-s)\right) \mathbb{F}_6(s, V_h(s))ds, \tag{5.8}$$

$$S_r(t) = e^{\left(-\frac{K_1(\alpha)}{K_0(\alpha)}t\right)}S_{r_0} + \frac{1}{K_0(\alpha)}\int_0^t (t-s)^{\alpha-1}\mathbb{E}_{1,\alpha}\left(-\frac{K_1(\alpha)}{K_0(\alpha)}(t-s)\right)\mathbb{F}_7(s, S_r(s))ds, \tag{5.9}$$

$$E_r(t) = e^{\left(-\frac{K_1(\alpha)}{K_0(\alpha)}t\right)}E_{r_0} + \frac{1}{K_0(\alpha)}\int_0^t (t-s)^{\alpha-1}\mathbb{E}_{1,\alpha}\left(-\frac{K_1(\alpha)}{K_0(\alpha)}(t-s)\right)\mathbb{F}_8(s, E_r(s))ds, \tag{5.10}$$

$$I_r(t) = e^{\left(-\frac{K_1(\alpha)}{K_0(\alpha)}t\right)}I_{r_0} + \frac{1}{K_0(\alpha)}\int_0^t (t-s)^{\alpha-1}\mathbb{E}_{1,\alpha}\left(-\frac{K_1(\alpha)}{K_0(\alpha)}(t-s)\right)\mathbb{F}_9(s, I_r(s))ds. \tag{5.11}$$

Define an operator $\mathcal{F} : \mathbb{X} \to \mathbb{X}$ where $\mathcal{F} = (\mathcal{F}_1, \mathcal{F}_2, \mathcal{F}_3, \mathcal{F}_4, \mathcal{F}_5, \mathcal{F}_6, \mathcal{F}_7, \mathcal{F}_8, \mathcal{F}_9)$. In consideration of (5.3) to (5.11), we obtain

$$\begin{aligned}
(\mathcal{F}_1 S_h)(t) &= e^{\left(-\frac{K_1(\alpha)}{K_0(\alpha)}t\right)}S_{h_0} + \frac{1}{K_0(\alpha)}\int_0^t (t-s)^{\alpha-1}\mathbb{E}_{1,\alpha}\left(-\frac{K_1(\alpha)}{K_0(\alpha)}(t-s)\right)\mathbb{F}_1(s, S_h(s))ds,\\
(\mathcal{F}_2 E_h)(t) &= e^{\left(-\frac{K_1(\alpha)}{K_0(\alpha)}t\right)}E_{h_0} + \frac{1}{K_0(\alpha)}\int_0^t (t-s)^{\alpha-1}\mathbb{E}_{1,\alpha}\left(-\frac{K_1(\alpha)}{K_0(\alpha)}(t-s)\right)\mathbb{F}_2(s, E_h(s))ds,\\
(\mathcal{F}_3 I_h)(t) &= e^{\left(-\frac{K_1(\alpha)}{K_0(\alpha)}t\right)}I_{h_0} + \frac{1}{K_0(\alpha)}\int_0^t (t-s)^{\alpha-1}\mathbb{E}_{1,\alpha}\left(-\frac{K_1(\alpha)}{K_0(\alpha)}(t-s)\right)\mathbb{F}_3(s, I_h(s))ds,\\
(\mathcal{F}_4 C_h)(t) &= e^{\left(-\frac{K_1(\alpha)}{K_0(\alpha)}t\right)}C_{h_0} + \frac{1}{K_0(\alpha)}\int_0^t (t-s)^{\alpha-1}\mathbb{E}_{1,\alpha}\left(-\frac{K_1(\alpha)}{K_0(\alpha)}(t-s)\right)\mathbb{F}_4(s, C_h(s))ds,\\
(\mathcal{F}_5 R_h)(t) &= e^{\left(-\frac{K_1(\alpha)}{K_0(\alpha)}t\right)}R_{h_0} + \frac{1}{K_0(\alpha)}\int_0^t (t-s)^{\alpha-1}\mathbb{E}_{1,\alpha}\left(-\frac{K_1(\alpha)}{K_0(\alpha)}(t-s)\right)\mathbb{F}_5(s, R_h(s))ds,\\
(\mathcal{F}_6 V_h)(t) &= e^{\left(-\frac{K_1(\alpha)}{K_0(\alpha)}t\right)}V_{h_0} + \frac{1}{K_0(\alpha)}\int_0^t (t-s)^{\alpha-1}\mathbb{E}_{1,\alpha}\left(-\frac{K_1(\alpha)}{K_0(\alpha)}(t-s)\right)\mathbb{F}_6(s, V_h(s))ds,\\
(\mathcal{F}_7 S_r)(t) &= e^{\left(-\frac{K_1(\alpha)}{K_0(\alpha)}t\right)}S_{r_0} + \frac{1}{K_0(\alpha)}\int_0^t (t-s)^{\alpha-1}\mathbb{E}_{1,\alpha}\left(-\frac{K_1(\alpha)}{K_0(\alpha)}(t-s)\right)\mathbb{F}_7(s, S_r(s))ds,\\
(\mathcal{F}_8 E_r)(t) &= e^{\left(-\frac{K_1(\alpha)}{K_0(\alpha)}t\right)}E_{r_0} + \frac{1}{K_0(\alpha)}\int_0^t (t-s)^{\alpha-1}\mathbb{E}_{1,\alpha}\left(-\frac{K_1(\alpha)}{K_0(\alpha)}(t-s)\right)\mathbb{F}_8(s, E_r(s))ds,\\
(\mathcal{F}_9 I_r)(t) &= e^{\left(-\frac{K_1(\alpha)}{K_0(\alpha)}t\right)}I_{r_0} + \frac{1}{K_0(\alpha)}\int_0^t (t-s)^{\alpha-1}\mathbb{E}_{1,\alpha}\left(-\frac{K_1(\alpha)}{K_0(\alpha)}(t-s)\right)\mathbb{F}_9(s, I_r(s))ds.
\end{aligned}$$

Next, the transformation of the $\mathbb{CPC}$-$\mathbb{MPOX}$ model (3.2) to $\mathcal{Y} = \mathcal{F}\mathcal{Y}$ that is a fixed point problem, will be later applied with a fixed point theory to prove that the $\mathbb{CPC}$-$\mathbb{MPOX}$ model (3.2) has a solution.

Theorem 5.1. *Suppose that $\mathbb{F} \in \mathbb{X}$ corresponding with the assumption (A_1) is as follows:*

(A_1) *There is a constant $\mathcal{N}_{\max} = \max\{\mathcal{N}_1, \mathcal{N}_2, \mathcal{N}_3, \mathcal{N}_4, \mathcal{N}_5, \mathcal{N}_6, \mathcal{N}_7, \mathcal{N}_8, \mathcal{N}_9\} > 0$, such that*

$$\begin{cases}
\Big|\mathbb{F}_i(t, S_h(t), E_h(t), I_h(t), C_h(t), R_h(t), V_h(t), S_r(t), E_r(t), I_r(t))\\
\qquad -\mathbb{F}_i(t, S_h^*(t), E_h^*(t), I_h^*(t), C_h^*(t), R_h^*(t), V_h^*(t), S_r^*(t), E_r^*(t)), I_r^*(t))\Big|\\
\leq \mathcal{N}_i\Big(\big|S_h(t) - S_h^*(t)\big| + \big|E_h(t) - E_h^*(t)\big| + \big|I_h(t) - I_h^*(t)\big|\\
\qquad + \big|C_h(t) - C_h^*(t)\big| + \big|R_h(t) - R_h^*(t)\big| + \big|V_h(t) - V_h^*(t)\big|\\
\qquad + \big|S_r(t) - S_r^*(t)\big| + \big|E_r(t) - E_r^*(t)\big| + \big|I_r(t) - I_r^*(t)\big|\Big),
\end{cases}$$

where $i = 1, 2, 3, \ldots, 9$ and S_h, E_h, I_h, C_h, R_h, V_h, S_r, E_r, $I_r \in \mathbb{X}$, and $t \in [0, T]$.

If

$$K_1(\alpha)\left[K_0^2(\alpha)\right]^{-1}\mathcal{N}_{\max} < 1, \tag{5.12}$$

then the $\mathbb{CPC}$-$\mathbb{MPOX}$ *model* (3.2) *has a unique solution.*

Proof. Define a bounded, closed, and convex subset $D_{r_a} := \{(S_h, E_h, I_h, C_h, R_h, V_h, S_r, E_r, I_r) \in \mathbb{X} : \|(S_h, E_h, I_h, C_h, R_h, V_h, S_r, E_r, I_r)\| \leq r_a\}$ with a radius r_a defined as

$$r_a \geq \mathcal{K}_{\max} + \frac{K_1(\alpha)}{K_0^2(\alpha)}\mathbb{F}^*_{\max}\left[1 - \frac{K_1(\alpha)}{K_0^2(\alpha)}\mathcal{N}_{\max}\right]^{-1},$$

where $\mathcal{K}_{\max} = \max\{S_{h_0}, E_{h_0}, I_{h_0}, C_{h_0}, R_{h_0}, V_{h_0}, S_{r_0}, E_{r_0}, I_{r_0}\}$ and $\mathbb{F}^*_{\max} = \max\{\mathbb{F}^*_1, \mathbb{F}^*_2, \mathbb{F}^*_3, \mathbb{F}^*_4, \mathbb{F}^*_5, \mathbb{F}^*_6, \mathbb{F}^*_7, \mathbb{F}^*_8, \mathbb{F}^*_9\}$. Let $\sup_{t\in[0,T]}|\mathbb{F}_i(s,0)| = \mathbb{F}^*_i < +\infty$, $i = 1, 2, 3, \ldots, 9$. The process is divided into two parts.

Step I. We prove that $\mathcal{F}D_{r_a} \subset D_{r_a}$.

For any $(S_h(t), E_h(t), I_h(t), C_h(t), R_h(t), V_h(t), S_r(t), E_r(t), I_r(t)) \in D_{r_a}$, $t \in [0, T]$, we have

$$\begin{aligned}
|(\mathcal{F}_1 S_h)(t)| &\leq \left|e^{\left(-\frac{K_1(\alpha)}{K_0(\alpha)}t\right)}S_{h_0}\right| + \frac{1}{K_0(\alpha)}\int_0^t (t-s)^{\alpha-1}\mathbb{E}_{1,\alpha}\left(-\frac{K_1(\alpha)}{K_0(\alpha)}(t-s)\right)\\
&\quad\times\Big[|\mathbb{F}_1(s, S_h(s)) - \mathbb{F}_1(s,0)| + |\mathbb{F}_1(s,0)|\Big]ds\\
&\leq S_{h_0} + \frac{1}{K_0(\alpha)}\int_0^t (t-s)^{\alpha-1}\mathbb{E}_{1,\alpha}\left(-\frac{K_1(\alpha)}{K_0(\alpha)}(t-s)\right)\Big[\mathcal{N}_1\Big[|S_h(t)| + |E_h(t)|\\
&\quad + |I_h(t)| + |C_h(t)| + |R_h(t)| + |V_h(t) + |S_r(t)| + |E_r(t)| + |I_r(t)|\Big] + \mathbb{F}^*_1\Big]ds\\
&\leq S_{h_0} + \frac{K_1(\alpha)}{K_0^2(\alpha)}\Big[\mathcal{N}_1\Big(|S_h(t)| + |E_h(t) + |I_h(t)| + |C_h(t)||\\
&\quad + |R_h(t)| + |V_h(t) + |S_r(t)| + |E_r(t)| + |I_r(t)|\Big) + \mathbb{F}^*_1\Big]\\
&\leq S_{h_0} + \frac{K_1(\alpha)}{K_0^2(\alpha)}\left[\mathcal{N}_1 r_a + \mathbb{F}^*_1\right].
\end{aligned}$$

In the same process, we also have

$$\begin{aligned}
|(\mathcal{F}_2 E_h)(t)| &\leq E_{h_0} + \frac{K_1(\alpha)}{K_0^2(\alpha)}\left[\mathcal{N}_2 r_a + \mathbb{F}^*_2\right],\\
|(\mathcal{F}_3 I_h)(t)| &\leq I_{h_0} + \frac{K_1(\alpha)}{K_0^2(\alpha)}\left[\mathcal{N}_3 r_a + \mathbb{F}^*_3\right],\\
|(\mathcal{F}_4 C_h)(t)| &\leq C_{h_0} + \frac{K_1(\alpha)}{K_0^2(\alpha)}\left[\mathcal{N}_4 r_a + \mathbb{F}^*_4\right],\\
|(\mathcal{F}_5 R_h)(t)| &\leq R_{h_0} + \frac{K_1(\alpha)}{K_0^2(\alpha)}\left[\mathcal{N}_5 r_a + \mathbb{F}^*_5\right],\\
|(\mathcal{F}_6 V_h)(t)| &\leq V_{h_0} + \frac{K_1(\alpha)}{K_0^2(\alpha)}\left[\mathcal{N}_6 r_a + \mathbb{F}^*_6\right],\\
|(\mathcal{F}_7 S_r)(t)| &\leq S_{r_0} + \frac{K_1(\alpha)}{K_0^2(\alpha)}\left[\mathcal{N}_7 r_a + \mathbb{F}^*_7\right],
\end{aligned}$$

$$
\begin{aligned}
|(\mathcal{F}_8 E_r)(t)| &\leq E_{r_0} + \frac{K_1(\alpha)}{K_0^2(\alpha)}\left[\mathcal{N}_8 r_a + \mathbb{F}_8^*\right], \\
|(\mathcal{F}_9 I_r)(t)| &\leq I_{r_0} + \frac{K_1(\alpha)}{K_0^2(\alpha)}\left[\mathcal{B}_9 r_a + \mathbb{F}_9^*\right].
\end{aligned}
$$

This yields that

$$
\|(\mathcal{F}\mathcal{Y})(t)\| \leq \mathcal{K}_{\max} + \frac{K_1(\alpha)}{K_0^2(\alpha)}\left[\mathcal{N}_{\max} r_a + \mathbb{F}_{\max}^*\right].
$$

Therefore, $\mathcal{F} D_{r_a} \subset D_{r_a}$.

Step II. We prove that $\mathcal{F}$ is a contraction.

Let $(S_h, E_h, I_h, C_h, R_h, V_h, S_r, E_r, I_r) \in D_{r_a}$ and $(S_h^*, E_h^*, I_h^*, C_h^*, R_h^*, V_h^*, S_r^*, E_r^*, I_r^*) \in D_{r_a}$, for $t \in [0, T]$. We obtain that

$$
\begin{aligned}
& |(\mathcal{F}_1 S_h)(t) - (\mathcal{F}_1 S_h^*)(t)| \\
\leq\ & \frac{1}{K_0(\alpha)} \int_0^t (t-s)^{\alpha-1} \mathbb{E}_{1,\alpha}\left(-\frac{K_1(\alpha)}{K_0(\alpha)}(t-s)\right) |\mathbb{F}_1(s, S_h(s)) - \mathbb{F}_1(s, S_h^*(s))| ds \\
\leq\ & \frac{1}{K_0(\alpha)} \int_0^t (t-s)^{\alpha-1} \mathbb{E}_{1,\alpha}\left(-\frac{K_1(\alpha)}{K_0(\alpha)}(t-s)\right) ds \times \mathcal{N}_1 \Big\{ |S_h(t) - S_h^*(t)| \\
& + |E_h(t) - E_h^*(t)| + |I_h(t) - I_h^*(t)| + |C_h(t) - C_h^*(t)| + |R_h(t) - R_h^*(t)| \\
& + |V_h(t) - V_h^*(t)| + |S_r(t) - S_r^*(t)| + |E_r(t) - E_r^*(t)| + |I_r(t) - I_r^*(t)| \Big\}.
\end{aligned}
$$

This yields that,

$$
|(\mathcal{F}_1 S_h)(t) - (\mathcal{F}_1 S_h^*)(t)| \leq \frac{K_1(\alpha)}{K_0^2(\alpha)} \mathcal{N}_1 \|\mathcal{Y}(t) - \bar{\mathcal{Y}}(t)\|.
$$

Likewise, we obtain

$$
\begin{aligned}
|(\mathcal{F}_2 E_h)(t) - (\mathcal{F}_2 E_h^*)(t)| &\leq \frac{K_1(\alpha)}{K_0^2(\alpha)} \mathcal{N}_2 \|\mathcal{Y}(t) - \bar{\mathcal{Y}}(t)\|, \\
|(\mathcal{F}_3 I_h)(t) - (\mathcal{F}_3 I_h^*)(t)| &\leq \frac{K_1(\alpha)}{K_0^2(\alpha)} \mathcal{N}_3 \|\mathcal{Y}(t) - \bar{\mathcal{Y}}(t)\|, \\
|(\mathcal{F}_4 C_h)(t) - (\mathcal{F}_4 C_h^*)(t)| &\leq \frac{K_1(\alpha)}{K_0^2(\alpha)} \mathcal{N}_4 \|\mathcal{Y}(t) - \bar{\mathcal{Y}}(t)\|, \\
|(\mathcal{F}_5 R_h)(t) - (\mathcal{F}_5 R_h^*)(t)| &\leq \frac{K_1(\alpha)}{K_0^2(\alpha)} \mathcal{N}_5 \|\mathcal{Y}(t) - \bar{\mathcal{Y}}(t)\|, \\
|(\mathcal{F}_6 V_h)(t) - (\mathcal{F}_6 V_h^*)(t)| &\leq \frac{K_1(\alpha)}{K_0^2(\alpha)} \mathcal{N}_6 \|\mathcal{Y}(t) - \bar{\mathcal{Y}}(t)\|, \\
|(\mathcal{F}_7 S_r)(t) - (\mathcal{F}_7 S_r^*)(t)| &\leq \frac{K_1(\alpha)}{K_0^2(\alpha)} \mathcal{N}_7 \|\mathcal{Y}(t) - \bar{\mathcal{Y}}(t)\|, \\
|(\mathcal{F}_8 E_r)(t) - (\mathcal{F}_8 E_r^*)(t)| &\leq \frac{K_1(\alpha)}{K_0^2(\alpha)} \mathcal{N}_8 \|\mathcal{Y}(t) - \bar{\mathcal{Y}}(t)\|, \\
|(\mathcal{F}_9 I_r)(t) - (\mathcal{F}_9 I_r^*)(t)| &\leq \frac{K_1(\alpha)}{K_0^2(\alpha)} \mathcal{N}_9 \|\mathcal{Y}(t) - \bar{\mathcal{Y}}(t)\|.
\end{aligned}
$$

Since $\mathcal{F} = (\mathcal{F}_1, \mathcal{F}_2, \mathcal{F}_3, \mathcal{F}_4, \mathcal{F}_5, \mathcal{F}_6, \mathcal{F}_7, \mathcal{F}_8, \mathcal{F}_9)$ and $\mathcal{N}_{\max} > 0$, then

$$\|\mathcal{F}(S_h, E_h, I_h, Q_h, R_h, S_r, E_r, I_r) - \mathcal{F}(S_h^*, E_h^*, I_h^*, Q_h^*, R_h^*, S_r^*, E_r^*, I_r^*)\| \leq \frac{K_1(\alpha)}{K_0^2(\alpha)} \mathcal{N}_{\max} \|\mathcal{Y}(t) - \bar{\mathcal{Y}}(t)\|.$$

Under the assumption (5.12), we can conclude that $\mathcal{F}$ is a contraction. Then, we get $\mathcal{F}$ has a unique fixed point. Therefore, the $\mathbb{CPC}$-$\mathbb{MPOX}$ model (3.2) has a unique solution. □

Next, we investigate some sufficient criteria of the Ulam's stability for the $\mathbb{CPC}$-$\mathbb{MPOX}$ model (3.2). The definitions of these types and some necessary remarks are provided below.

Assume that $\kappa_{\mathbb{F}_\mathcal{Y}} > 0$ is a constant and $P_{\mathbb{F}_\mathcal{Y}} \in C([0, T], \mathbb{R}^+)$. The inequalities are given:

$$\left|{}^{\mathbb{CPC}}\mathfrak{D}_{0,t}^{\alpha} \mathcal{Y}(t) - \mathbb{F}(t, \mathcal{Y}(t))\right| \leq \kappa_{\mathbb{F}_\mathcal{Y}}, \tag{5.13}$$

$$\left|{}^{\mathbb{CPC}}\mathfrak{D}_{0,t}^{\alpha} \mathcal{Y}(t) - \mathbb{F}(t, \mathcal{Y}(t))\right| \leq \kappa_{\mathbb{F}_\mathcal{Y}} P_{\mathbb{F}_\mathcal{Y}}(t), \tag{5.14}$$

$$\left|{}^{\mathbb{CPC}}\mathfrak{D}_{0,t}^{\alpha} \mathcal{Y}(t) - \mathbb{F}(t, \mathcal{Y}(t))\right| \leq P_{\mathbb{F}_\mathcal{Y}}(t), \tag{5.15}$$

where $t \in [0, T]$ and $\kappa_{\mathbb{F}_\mathcal{Y}} = \max(\kappa_{\mathbb{F}_{\mathcal{Y}_j}})^T$, for $j = 1, 2, \ldots, 9$.

Definition 5.2. *The $\mathbb{CPC}$-$\mathbb{MPOX}$ model* (3.2) *is called $\mathbb{UH}$ stable if there exists a constant $\Phi_{\mathbb{F}_\mathcal{Y}} > 0$ such that for every $\kappa_{\mathbb{F}_\mathcal{Y}} > 0$ and each solution $Z_\mathcal{Y} \in \mathbb{X}$ of* (5.13)*, there exist a solution $\mathcal{Y} \in \mathbb{X}$ of* (3.2) *with*

$$|Z_\mathcal{Y}(t) - \mathcal{Y}(t)| \leq \Phi_{\mathbb{F}_\mathcal{Y}} \kappa_{\mathbb{F}_\mathcal{Y}}, \tag{5.16}$$

where $t \in [0, T]$ and $\Phi_{\mathbb{F}_\mathcal{Y}} = \max(\Phi_{\mathbb{F}_{\mathcal{Y}_i}})^T$, $i = 1, 2, \ldots, 9$.

Definition 5.3. *The $\mathbb{CPC}$-$\mathbb{MPOX}$ model* (3.2) *is called generalized $\mathbb{UH}$ stable if there exists a function $P_{\mathbb{F}_\mathcal{Y}} \in C([0, T], \mathbb{R}^+)$, with $P_{\mathbb{F}_\mathcal{Y}}(0) = 0$ so that for $\kappa_{\mathbb{F}_\mathcal{Y}} > 0$ and for each solution $Z_\mathcal{Y} \in \mathbb{X}$ of* (5.14)*, there exist a solution $\mathcal{Y} \in \mathbb{X}$ of* (3.2) *with*

$$|Z_\mathcal{Y}(t) - \mathcal{Y}(t)| \leq P_{\mathbb{F}_\mathcal{Y}}(\kappa_{\mathbb{F}_\mathcal{Y}}), \tag{5.17}$$

where $t \in [0, T]$, and $P_{\mathbb{F}_\mathcal{Y}} = \max(P_{\mathbb{F}_\mathcal{Y}})^T$, $i = 1, 2, \ldots, 9$.

Definition 5.4. *The $\mathbb{CPC}$-$\mathbb{MPOX}$ model* (3.2) *is called $\mathbb{UHR}$ stable with respect to $P_{\mathbb{F}_\mathcal{Y}} \in C([0, T], \mathbb{R}^+)$ if there exists a number $\Omega_{\mathbb{F}_\mathcal{Y}} > 0$ so that for every $\kappa_{\mathbb{F}_\mathcal{Y}} > 0$ and for each solution $Z_\mathcal{Y} \in \mathbb{X}$ of* (5.15)*, there exists a solution $\mathcal{Y} \in \mathbb{X}$ of* (3.2) *with*

$$|Z_\mathcal{Y}(t) - \mathcal{Y}(t)| \leq \Omega_{\mathbb{F}_\mathcal{Y}} \kappa_{\mathbb{F}_\mathcal{Y}} P_{\mathbb{F}_\mathcal{Y}}(t), \tag{5.18}$$

where $t \in [0, T]$, $\Omega_{\mathbb{F}_\mathcal{Y}} = \max(\Omega_{\mathbb{F}_{\mathcal{Y}_i}})^T$, and $P_{\mathbb{F}_\mathcal{Y}} = \max(P_{\mathbb{F}_{\mathcal{Y}_i}})^T$, $i = 1, 2, \ldots, 9$.

Definition 5.5. *The $\mathbb{CPC}$-$\mathbb{MPOX}$ model* (3.2) *is called generalized $\mathbb{UHR}$ stable with respect to $P_{\mathbb{F}_\mathcal{Y}} \in C([0, T], \mathbb{R}^+)$ if there exists a number $\Omega_{\mathbb{F}_\mathcal{Y}} > 0$ so that for each solution $Z_\mathcal{Y} \in \mathbb{X}$ of* (5.15)*, there exists a solution $\mathcal{Y} \in \mathbb{X}$ of* (3.2) *with*

$$|Z_\mathcal{Y}(t) - \mathcal{Y}(t)| \leq \Omega_{\mathbb{F}_\mathcal{Y}} P_{\mathbb{F}_\mathcal{Y}}(t), \tag{5.19}$$

where $t \in [0, T]$, $\Omega_{\mathbb{F}_\mathcal{Y}} = \max(\Omega_{\mathbb{F}_{\mathcal{Y}_i}})^T$, and $P_{\mathbb{F}_\mathcal{Y}} = \max(P_{\mathbb{F}_{\mathcal{Y}_i}})^T$, $i = 1, 2, \ldots, 9$.

Remark 5.6. *$Z_\mathcal{Y} \in \mathbb{X}$ is the solution of* (5.13)*, if and only if, there is $\chi_\mathcal{Y}(0) = 0$ satisfied $|\chi_\mathcal{Y}(t)| \leq \kappa_{\mathbb{G}_\mathcal{Y}}$, $\chi_\mathcal{Y} = \max(\chi_{\mathcal{Y}_i})^T, i = 1, 2, \ldots, 9$, $\kappa_{F_\mathcal{Y}} > 0$, and ${}^{\mathbb{CPC}}\mathfrak{D}_{0,t}^{\alpha} \mathcal{Y}(t) = \mathbb{F}(t, \mathcal{Y}(t)) + \chi_\mathcal{Y}(t)$.*

Remark 5.7. *$Z_{\mathcal{Y}} \in \mathbb{X}$ is the solution of* (5.14)*, if and only if, there is $\psi_{\mathcal{Y}} \in \mathbb{X}$ satisfied $|\psi_{\mathcal{Y}}(t)| \leq \kappa_{\mathbb{F}_{\mathcal{Y}}} P_{\mathbb{F}_{\mathcal{Y}}}(t)$, $\psi_{\mathcal{Y}} = \max(\psi_{\mathcal{Y}_i})^T$, $P_{\mathbb{F}_{\mathcal{Y}}} = \max(P_{\mathbb{F}_{\mathcal{Y}_i}})^T$, $i = 1, 2, \ldots, 9$, and ${}^{\mathbb{CPC}}\mathfrak{D}^{\alpha}_{0,t}\mathcal{Y}(t) = \mathbb{F}(t, \mathcal{Y}(t)) + \psi_{\mathcal{Y}}(t)$.*

Lemma 5.8. *Assume that $Z_{\mathcal{Y}} \in \mathbb{X}$ is a solution of* (5.13)*, then*

$$\left| Z_{\mathcal{Y}}(t) - Z_{\mathcal{Y}_0} - \frac{1}{K_0(\alpha)} \int_0^t (t-s)^{\alpha-1} \mathbb{E}_{1,\alpha}\left(-\frac{K_1(\alpha)}{K_0(\alpha)}(t-s)\right) \mathbb{F}(s, Z_{\mathcal{Y}}(s)) ds \right| \leq \frac{\kappa_{\mathbb{F}_{\mathcal{Y}}} K_1(\alpha)}{(K_0(\alpha))^2}. \tag{5.20}$$

Proof. Let $Z_{\mathcal{Y}}$ be the solution of (5.13). From Remark (5.6), we have

$$\begin{cases} {}^{\mathbb{CPC}}\mathfrak{D}^{\alpha}_{0,t} Z(t) = \mathbb{F}(t, Z(t)) + \chi_{\mathcal{Y}}(t), \\ Z_{\mathcal{Y}}(0) = Z_{\mathcal{Y}_0} \geq 0. \end{cases} \tag{5.21}$$

Thus, the solution to (5.21) is provided below:

$$\begin{aligned} Z_{\mathcal{Y}}(t) &= Z_{\mathcal{Y}_0} + \frac{1}{K_0(\alpha)} \int_0^t (t-s)^{\alpha-1} \mathbb{E}_{1,\alpha}\left(-\frac{K_1(\alpha)}{K_0(\alpha)}(t-s)\right) \mathbb{F}(s, Z_{\mathcal{Y}}(s)) ds \\ &\quad + \frac{1}{K_0(\alpha)} \int_0^t (t-s)^{\alpha-1} \mathbb{E}_{1,\alpha}\left(-\frac{K_1(\alpha)}{K_0(\alpha)}(t-s)\right) \chi_{\mathcal{Y}}(s) ds. \end{aligned}$$

Therefore,

$$\begin{aligned} &\left| Z_{\mathcal{Y}}(t) - Z_{\mathcal{Y}_0} - \frac{1}{K_0(\alpha)} \int_0^t (t-s)^{\alpha-1} \mathbb{E}_{1,\alpha}\left(-\frac{K_1(\alpha)}{K_0(\alpha)}(t-s)\right) \mathbb{F}(s, Z_{\mathcal{Y}}(s)) ds \right| \\ \leq\ & \frac{1}{K_0(\alpha)} \int_0^t (t-s)^{\alpha-1} \mathbb{E}_{1,\alpha}\left(-\frac{K_1(\alpha)}{K_0(\alpha)}(t-s)\right) \chi_{\mathcal{Y}}(s) ds \leq \frac{K_1(\alpha)}{(K_0(\alpha))^2} \kappa_{\mathbb{F}_{\mathcal{Y}}}. \end{aligned}$$

The proof is completed. □

Theorem 5.9. *Assume the conditions in Theorem 5.1 and Lemma 5.8 are satisfied, then the $\mathbb{CPC}$-$\mathbb{MPOX}$ model* (3.2) *is $\mathbb{UH}$ stable.*

Proof. Assume that $\kappa_{\mathbb{F}_{\mathcal{Y}}} \in \mathbb{R}^+$ and $Z_{\mathcal{Y}}$ is a solution of (5.13). Let $\mathcal{Y} \in \mathbb{X}$ be a unique solution of (3.2), then

$$\begin{aligned} |Z_{\mathcal{Y}}(t) - \mathcal{Y}(t)| &\leq \left| Z_{\mathcal{Y}}(t) - Z_{\mathcal{Y}_0} - \frac{1}{K_0(\alpha)} \int_0^t (t-s)^{\alpha-1} \mathbb{E}_{1,\alpha}\left(-\frac{K_1(\alpha)}{K_0(\alpha)}(t-s)\right) \mathbb{F}(s, Z_{\mathcal{Y}}(s)) ds \right| \\ &\quad + \frac{1}{K_0(\alpha)} \int_0^t (t-s)^{\alpha-1} \mathbb{E}_{1,\alpha}\left(-\frac{K_1(\alpha)}{K_0(\alpha)}(t-s)\right) |\mathbb{F}(s, Z_{\mathcal{Y}}(s)) - \mathbb{F}(s, \mathcal{Y}(t))| ds \\ &\leq \frac{K_1(\alpha)}{(K_0(\alpha))^2} \left(\kappa_{\mathbb{F}_{\mathcal{Y}}} + \mathcal{N}_{\max} |Z_{\mathcal{Y}}(t) - \mathcal{Y}(t)|\right). \end{aligned}$$

Setting

$$\Phi_{\mathbb{F}_{\mathcal{Y}}} := \frac{K_1(\alpha)}{(K_0(\alpha))^2}\left(1 - \frac{K_1(\alpha)}{(K_0(\alpha))^2}\mathcal{N}_{\max}\right)^{-1},$$

this yields that $|Z_{\mathcal{Y}}(t) - \mathcal{Y}(t)| \leq \Phi_{\mathbb{F}_{\mathcal{Y}}}\kappa_{\mathbb{F}_{\mathcal{Y}}}$. Hence, by Definition 5.2, the $\mathbb{CPC}$-$\mathbb{MPOX}$ model (3.2) is $\mathbb{UH}$ stable. □

Corollary 5.10. *Setting $P_{\mathbb{F}_{\mathcal{Y}}}(\kappa_{\mathbb{F}_{\mathcal{Y}}}) = \Phi_{\mathbb{F}_{\mathcal{Y}}}\kappa_{\mathbb{F}_{\mathcal{Y}}}$ with $P_{\mathbb{F}_{\mathcal{Y}}}(0) = 0$ in Theorem 5.9, by Definition 5.3, the $\mathbb{CPC}$-$\mathbb{MPOX}$ model* (3.2) *is $\mathbb{UH}$ stable.*

The following conditions are necessary to prove the $\mathbb{UHR}$ and generalized $\mathbb{UHR}$ stability.

(D_1) There is an increasing function $P_{\mathbb{F}_{\mathcal{Y}}} \in C([0,T],\mathbb{R}^+)$ and a number $\lambda_{\mathbb{F}_{\mathcal{Y}}} > 0$, so that

$${}^{\mathbb{CPC}}I_0^{\alpha} P_{\mathbb{F}_{\mathcal{Y}}}(t) \leq \lambda_{\mathbb{F}_{\mathcal{Y}}} P_{\mathbb{F}_{\mathcal{Y}}}(t).$$

Lemma 5.11. *Let $Z_{\mathcal{Y}} \in \mathbb{X}$ be the solution of* (5.15)*, then*

$$\left|Z_{\mathcal{Y}}(t) - Z_{\mathcal{Y}_0} - \frac{1}{K_0(\alpha)}\int_0^t (t-s)^{\alpha-1}\mathbb{E}_{1,\alpha}\left(-\frac{K_1(\alpha)}{K_0(\alpha)}(t-s)\right)\mathbb{F}(s, Z_{\mathcal{Y}}(s))ds\right| \leq \kappa_{\mathbb{F}_{\mathcal{Y}}}\lambda_{\mathbb{F}_{\mathcal{Y}}}P_{\mathbb{F}_{\mathcal{Y}}}(t). \tag{5.22}$$

Proof. Let $Z_{\mathcal{Y}} \in \mathbb{X}$ be a solution of (5.15). Applying Remark 5.7, we obtain

$$\begin{cases} {}^{\mathbb{CPC}}\mathfrak{D}_{0,t}^{\alpha} Z(t) = \mathbb{F}(t, Z(t)) + \psi_{\mathcal{Y}}(t), \\ Z_{\mathcal{Y}}(0) = Z_{\mathcal{Y}_0} \geq 0. \end{cases} \tag{5.23}$$

Hence, a solution of (5.23) is provided below:

$$\begin{aligned} Z_{\mathcal{Y}}(t) &= Z_{\mathcal{Y}_0} + \frac{1}{K_0(\alpha)}\int_0^t (t-s)^{\alpha-1}\mathbb{E}_{1,\alpha}\left(-\frac{K_1(\alpha)}{K_0(\alpha)}(t-s)\right)\mathbb{F}(s, Z_{\mathcal{Y}}(s))ds \\ &\quad + \frac{1}{K_0(\alpha)}\int_0^t (t-s)^{\alpha-1}\mathbb{E}_{1,\alpha}\left(-\frac{K_1(\alpha)}{K_0(\alpha)}(t-s)\right)\psi_{\mathcal{Y}}(s)ds. \end{aligned}$$

Since,

$$\begin{aligned} &\left|Z_{\mathcal{Y}}(t) - Z_{\mathcal{Y}_0} - \frac{1}{K_0(\alpha)}\int_0^t (t-s)^{\alpha-1}\mathbb{E}_{1,\alpha}\left(-\frac{K_1(\alpha)}{K_0(\alpha)}(t-s)\right)\mathbb{F}(s, Z_{\mathcal{Y}}(s))ds\right| \\ \leq\ & \frac{1}{K_0(\alpha)}\int_0^t (t-s)^{\alpha-1}\mathbb{E}_{1,\alpha}\left(-\frac{K_1(\alpha)}{K_0(\alpha)}(t-s)\right)|\psi_{\mathcal{Y}}(s)|\,ds \leq \kappa_{\mathbb{F}_{\mathcal{Y}}}\lambda_{\mathbb{F}_{\mathcal{Y}}}P_{\mathbb{F}_{\mathcal{Y}}}(t), \end{aligned}$$

then, the inequality (5.22) is achieved. □

Theorem 5.12. *Assume the conditions in Theorem 5.1 and Lemma 5.11 are satisfied, then the $\mathbb{CPC}$-$\mathbb{MPOX}$ model* (3.2) *is $\mathbb{UHR}$ stable.*

Proof. Let $\kappa_{\mathbb{F}_{\mathcal{Y}}} \in \mathbb{R}^+$ and $Z_{\mathcal{Y}}$ be the solution of (5.15). Suppose that $\mathcal{Y} \in \mathbb{X}$ is a unique solution of the $\mathbb{CPC}$-$\mathbb{MPOX}$ model (3.2), then

$$\begin{aligned} |Z_{\mathcal{Y}}(t) - \mathcal{Y}(t)| &\leq \left| Z_{\mathcal{Y}}(t) - Z_{\mathcal{Y}_0} - \frac{1}{K_0(\alpha)} \int_0^t (t-s)^{\alpha-1} \mathbb{E}_{1,\alpha}\left(-\frac{K_1(\alpha)}{K_0(\alpha)}(t-s)\right) \mathbb{F}(s, Z_{\mathcal{Y}}(s)) ds \right| \\ &\quad + \frac{1}{K_0(\alpha)} \int_0^t (t-s)^{\alpha-1} \mathbb{E}_{1,\alpha}\left(-\frac{K_1(\alpha)}{K_0(\alpha)}(t-s)\right) |\mathbb{F}(s, Z_{\mathcal{Y}}(s)) - \mathbb{F}(s, \mathcal{Y}(t))| \, ds \\ &\leq \kappa_{\mathbb{F}_{\mathcal{Y}}} \lambda_{\mathbb{F}_{\mathcal{Y}}} P_{\mathbb{F}_{\mathcal{Y}}}(t) + \frac{K_1(\alpha)}{(K_0(\alpha))^2} \mathcal{N}_{\max} |Z_{\mathcal{Y}}(t) - \mathcal{Y}(t)| . \end{aligned}$$

Setting

$$\Phi_{\mathbb{G}_{\mathcal{Y}}} := \lambda_{\mathbb{G}_{\mathcal{Y}}} \left(1 - \tfrac{K_1(\alpha)}{(K_0(\alpha))^2} \mathcal{M}_{\max}\right)^{-1},$$

this yields that $|Z_{\mathcal{Y}}(t) - \mathcal{Y}(t)| \leq \Phi_{\mathbb{F}_{\mathcal{Y}}} \kappa_{\mathbb{F}_{\mathcal{Y}}} P_{\mathbb{F}_{\mathcal{Y}}}(t)$. Hence, by Definition 5.4, the $\mathbb{CPC}$-$\mathbb{MPOX}$ model (3.2) is $\mathbb{UHR}$ stable. □

Corollary 5.13. *Setting $\kappa_{\mathbb{G}_{\mathcal{Y}}} = 1$ in Theorem 5.12, by Definition 5.5, the $\mathbb{CPC}$-$\mathbb{MPOX}$ model* (3.2) *is $\mathbb{UHR}$ stable.*

6. Numerical algorithm

This section derives the numerical schemes for solving the approximated solution of the $\mathbb{CPC}$-$\mathbb{MPOX}$ model (3.2) by utilizing the decomposition technique for the $\mathbb{CPC}$ derivative operator. Next, we create an approximation design for the $\mathbb{CPC}$ derivative operator via $\alpha \in (0, 1]$ of a function $f(t)$. We will make a sequence of $N+1$ equations under $N+1$ conditions for the fractional Cauchy problem in the context of $\mathbb{CPC}$ derivative operator [47]. A sequence (f_N) of the solutions to such systems eventually leads to the solution of the obtained problem.

Theorem 6.1. *Assume that N is a positive number and $f \in AC^2([0, T], \mathbb{R})$. Let*

$$A_N = \sum_{i=0}^{N} \frac{\Gamma(i + \alpha - 1)}{i!\Gamma(2-\alpha)\Gamma(\alpha - 1)}, \qquad B_{N,i} = \frac{\Gamma(i + \alpha - 1)}{(i-1)!\Gamma(2-\alpha)\Gamma(\alpha - 1)}, \tag{6.1}$$

$\mathcal{V}_i : [0, T] \to \mathbb{R}$ be functions defined by

$$\mathcal{V}_i(t) = \int_0^t s^{i-1} \left[Q^{\alpha} (1-\alpha) f(s) + \alpha Q^{1-\alpha} C^{2\alpha} f'(s) \right] ds. \tag{6.2}$$

Then,

$${}^{\mathbb{CPC}}\mathfrak{D}^{\alpha}_{0,t} f(t) = \frac{A_N}{t^{\alpha-1}} \left[Q^{\alpha} (1-\alpha) f(t) + \alpha Q^{1-\alpha} C^{2\alpha} f'(t) \right] - \sum_{i=1}^{N} t^{1-\alpha-i} B_{N,i} \mathcal{V}_i(t) + \mathcal{E}_{tr}(t), \tag{6.3}$$

where $\lim_{N\to\infty} \mathcal{E}_{tr}(t) = 0$ for $t \in [0, T]$.

Proof. Using Definition 2.3 and $\mathcal{K}_1(\alpha) = Q^\alpha(1-\alpha)$, $\mathcal{K}_0(\alpha) = \alpha Q^{1-\alpha}C^{2\alpha}$, $\alpha \in (0,1]$, we have

$$^{\mathbb{CPC}}\mathfrak{D}^{\alpha}_{0,t} f(t) = \frac{1}{\Gamma(1-\alpha)} \int_0^t \left[Q^\alpha(1-\alpha) f(s) + \alpha Q^{1-\alpha} C^{2\alpha} f'(s)\right](t-s)^{-\alpha} ds.$$

Let $u = Q^\alpha(1-\alpha) f(s) + \alpha Q^{1-\alpha} C^{2\alpha} f'(s)$ and $dv = (t-s)^{-\alpha} ds$. Using the integrating by part technique, yields that

$$\begin{aligned} ^{\mathbb{CPC}}\mathfrak{D}^{\alpha}_{0,t} f(t) &= \frac{t^{1-\alpha}}{\Gamma(2-\alpha)}\left[Q^\alpha(1-\alpha) f(0) + \alpha Q^{1-\alpha} C^{2\alpha} f'(0)\right] \\ &\quad + \frac{1}{\Gamma(2-\alpha)} \int_0^t (t-s)^{-\alpha+1} \frac{d}{ds}\left[Q^\alpha(1-\alpha) f(s) + \alpha Q^{1-\alpha} C^{2\alpha} f'(s)\right] ds. \end{aligned} \tag{6.4}$$

Applying the generalized binomial theorem, it follows that

$$(t-s)^{1-\alpha} = (t-a)^{1-\alpha}\left(1 - \frac{s-a}{t-a}\right)^{1-\alpha} = (t-a)^{1-\alpha} \sum_{i=0}^{\infty} \frac{\Gamma(i+\alpha-1)}{\Gamma(\alpha-1)\, i!}\left(\frac{s-a}{t-a}\right)^i. \tag{6.5}$$

Plugging (6.5) into (6.4), it follows that

$$\begin{aligned} &^{\mathbb{CPC}}\mathfrak{D}^{\alpha}_{0,t} f(t) \\ &= \mathcal{E}_{tr}(t) + \frac{t^{1-\alpha}}{\Gamma(2-\alpha)}\left[Q^\alpha(1-\alpha) f(0) + \alpha Q^{1-\alpha} C^{2\alpha} f'(0)\right] \\ &\quad + \frac{1}{\Gamma(2-\alpha)} \int_0^t t^{1-\alpha} \sum_{i=0}^{N} \frac{\Gamma(i+\alpha-1)}{\Gamma(\alpha-1)\, i!}\left(\frac{s}{t}\right)^i \frac{d}{ds}\left[Q^\alpha(1-\alpha) f(s) + \alpha Q^{1-\alpha} C^{2\alpha} f'(s)\right] ds, \end{aligned}$$

where

$$\begin{aligned} \mathcal{E}_{tr}(t) &= \frac{1}{\Gamma(2-\alpha)} \int_0^t t^{1-\alpha} R_N(s) \frac{d}{ds}\left[Q^\alpha(1-\alpha) f(s) + \alpha Q^{1-\alpha} C^{2\alpha} f'(s)\right] ds, \\ R_N(s) &= \sum_{i=N+1}^{\infty} \frac{\Gamma(i+\alpha-1)}{i!\Gamma(\alpha-1)}\left(\frac{s}{t}\right)^i. \end{aligned} \tag{6.6}$$

Hence, by direct calculation, we get

$$\begin{aligned} ^{\mathbb{CPC}}\mathfrak{D}^{\alpha}_{0,t} f(t) &= \mathcal{E}_{tr}(t) + \frac{t^{1-\alpha}}{\Gamma(2-\alpha)}\left[Q^\alpha(1-\alpha) f(0) + \alpha Q^{1-\alpha} C^{2\alpha} f'(0)\right] \\ &\quad + \frac{t^{1-\alpha}}{\Gamma(2-\alpha)} \sum_{i=0}^{N} \frac{\Gamma(i+\alpha-1)}{\Gamma(\alpha-1)\, i! t^i} \int_0^t s^i \frac{d}{ds}\left[Q^\alpha(1-\alpha) f(s) + \alpha Q^{1-\alpha} C^{2\alpha} f'(s)\right] ds \\ &= \mathcal{E}_{tr}(t) + \frac{t^{1-\alpha}}{\Gamma(2-\alpha)}\left[Q^\alpha(1-\alpha) f(0) + \alpha Q^{1-\alpha} C^{2\alpha} f'(0)\right] \\ &\quad + \frac{t^{1-\alpha}}{\Gamma(2-\alpha)} \int_0^t \frac{d}{ds}\left[Q^\alpha(1-\alpha) f(s) + \alpha Q^{1-\alpha} C^{2\alpha} f'(s)\right] ds \\ &\quad + \frac{t^{1-\alpha}}{\Gamma(2-\alpha)} \sum_{i=1}^{N} \frac{\Gamma(i+\alpha-1)}{\Gamma(\alpha-1)\, i! t^i} \int_0^t s^i \frac{d}{ds}\left[Q^\alpha(1-\alpha) f(s) + \alpha Q^{1-\alpha} C^{2\alpha} f'(s)\right] ds \end{aligned}$$

$$= \mathcal{E}_{tr}(t) + \frac{t^{1-\alpha}}{\Gamma(2-\alpha)}\left[Q^{\alpha}(1-\alpha)f(t) + \alpha Q^{1-\alpha}C^{2\alpha}f'(t)\right] + \frac{t^{1-\alpha}}{\Gamma(2-\alpha)}\sum_{i=1}^{N}\frac{\Gamma(i+\alpha-1)}{\Gamma(\alpha-1)\,i!t^{i}}\int_0^t s^{i}\frac{d}{ds}\left[Q^{\alpha}(1-\alpha)f(s) + \alpha Q^{1-\alpha}C^{2\alpha}f'(s)\right]ds.$$

Let $u = s^i$ and $dv = \frac{d}{ds}\left[Q^{\alpha}(1-\alpha)f(s) + \alpha Q^{1-\alpha}C^{2\alpha}f'(s)\right]ds$. Using the integrating by part technique, it follows that

$$\begin{aligned}
{}^{\mathbb{CPC}}\mathfrak{D}^{\alpha}_{0,t}f(t) &= \mathcal{E}_{tr}(t) + \frac{t^{1-\alpha}}{\Gamma(2-\alpha)}\left[Q^{\alpha}(1-\alpha)f(t) + \alpha Q^{1-\alpha}C^{2\alpha}f'(t)\right] \\
&\quad + \frac{t^{1-\alpha}}{\Gamma(2-\alpha)}\sum_{i=1}^{N}\frac{\Gamma(i+\alpha-1)\,t^{i}}{\Gamma(\alpha-1)\,i!t^{i}}\left[Q^{\alpha}(1-\alpha)f(t) + \alpha Q^{1-\alpha}C^{2\alpha}f'(t)\right] \\
&\quad - \frac{t^{1-\alpha}}{\Gamma(2-\alpha)}\sum_{i=1}^{N}\frac{\Gamma(i+\alpha-1)}{\Gamma(\alpha-1)\,i!t^{i}}\int_0^t is^{i-1}\left[Q^{\alpha}(1-\alpha)f(s) + \alpha Q^{1-\alpha}C^{2\alpha}f'(s)\right]ds \\
&= \mathcal{E}_{tr}(t) + \frac{t^{1-\alpha}}{\Gamma(2-\alpha)}\sum_{i=0}^{N}\frac{\Gamma(i+\alpha-1)}{\Gamma(\alpha-1)\,i!}\left[Q^{\alpha}(1-\alpha)f(t) + \alpha Q^{1-\alpha}C^{2\alpha}f'(t)\right] \\
&\quad - \frac{t^{1-\alpha}}{\Gamma(2-\alpha)}\sum_{i=1}^{N}\frac{\Gamma(i+\alpha-1)}{\Gamma(\alpha-1)\,i!t^{i}}\int_0^t is^{i-1}\left[Q^{\alpha}(1-\alpha)f(s) + \alpha Q^{1-\alpha}C^{2\alpha}f'(s)\right]ds.
\end{aligned}$$

Now, we show that $\mathcal{E}_{tr}(t) \to 0$ as $N \to \infty$ for $t \in [0,T]$, and to show this, we give an upper bound for the error term. Since $\Gamma(x+\alpha) \sim \Gamma(x)x^{\alpha}$ and $s/t < 1$,

$$|R_N(s)| = \sum_{i=N+1}^{\infty}\frac{\Gamma(i+\alpha-1)}{i!}\left(\frac{s}{t}\right)^{i} \le \sum_{i=N+1}^{\infty}\frac{\Gamma(i+\alpha-1)}{i!} \le \sum_{i=N+1}^{\infty} i^{\alpha-2} \le \int_N^{\infty} s^{\alpha-2}ds.$$

Then,

$$|R_N(s)| \le \frac{1}{N^{1-\alpha}(1-\alpha)}. \tag{6.7}$$

Substituting (6.7) into (6.6) with $M^*(t) = \max_{s\in[0,T]}\left|\frac{d}{ds}\left[Q^{\alpha}(1-\alpha)f(s) + \alpha Q^{1-\alpha}C^{2\alpha}f'(s)\right]\right|$ implies the following upper bound:

$$|\mathcal{E}_{tr}(t)| \le \frac{t^{2-\alpha}M^*(t)}{N^{1-\alpha}(1-\alpha)\Gamma(2-\alpha)}. \tag{6.8}$$

The righthand side of (6.8) tends to zero for all $t \in (0,T)$ as $N \to \infty$. □

To obtain the numerical approximation of the $\mathbb{CPC}$-$\mathbb{MPOX}$ model (3.2), we apply Theorem 6.1. Then,

$$\begin{aligned}
{}^{\mathbb{CPC}}\mathfrak{D}^{\alpha}_{0,t}S_h(t) &= \frac{A_N}{t^{\alpha-1}}\left[Q^{\alpha}(1-\alpha)S_h(t) + \alpha Q^{1-\alpha}C^{2\alpha}S_h'(t)\right] - \sum_{i=1}^{N} t^{1-\alpha-i}B_{N,i}\mathcal{V}_{S_{h_i}}(t), \\
{}^{\mathbb{CPC}}\mathfrak{D}^{\alpha}_{0,t}E_h(t) &= \frac{A_N}{t^{\alpha-1}}\left[Q^{\alpha}(1-\alpha)E_h(t) + \alpha Q^{1-\alpha}C^{2\alpha}E_h'(t)\right] - \sum_{i=1}^{N} t^{1-\alpha-i}B_{N,i}\mathcal{V}_{E_{h_i}}(t),
\end{aligned}$$

$$
\begin{aligned}
{}^{\mathbb{CPC}}\mathfrak{D}^{\alpha}_{0,t} I_h(t) &= \frac{A_N}{t^{\alpha-1}}\left[Q^{\alpha}(1-\alpha) I_h(t) + \alpha Q^{1-\alpha} C^{2\alpha} I'_h(t)\right] - \sum_{i=1}^{N} t^{1-\alpha-i} B_{N,i} \mathcal{V}_{I_{h_i}}(t),\\
{}^{\mathbb{CPC}}\mathfrak{D}^{\alpha}_{0,t} C_h(t) &= \frac{A_N}{t^{\alpha-1}}\left[Q^{\alpha}(1-\alpha) C_h(t) + \alpha Q^{1-\alpha} C^{2\alpha} C'_h(t)\right] - \sum_{i=1}^{N} t^{1-\alpha-i} B_{N,i} \mathcal{V}_{C_{h_i}}(t),\\
{}^{\mathbb{CPC}}\mathfrak{D}^{\alpha}_{0,t} R_h(t) &= \frac{A_N}{t^{\alpha-1}}\left[Q^{\alpha}(1-\alpha) R_h(t) + \alpha Q^{1-\alpha} C^{2\alpha} R'_h(t)\right] - \sum_{i=1}^{N} t^{1-\alpha-i} B_{N,i} \mathcal{V}_{R_{h_i}}(t),\\
{}^{\mathbb{CPC}}\mathfrak{D}^{\alpha}_{0,t} V_h(t) &= \frac{A_N}{t^{\alpha-1}}\left[Q^{\alpha}(1-\alpha) V_h(t) + \alpha Q^{1-\alpha} C^{2\alpha} V'_h(t)\right] - \sum_{i=1}^{N} t^{1-\alpha-i} B_{N,i} \mathcal{V}_{V_{h_i}}(t),\\
{}^{\mathbb{CPC}}\mathfrak{D}^{\alpha}_{0,t} S_r(t) &= \frac{A_N}{t^{\alpha-1}}\left[Q^{\alpha}(1-\alpha) S_r(t) + \alpha Q^{1-\alpha} C^{2\alpha} S'_r(t)\right] - \sum_{i=1}^{N} t^{1-\alpha-i} B_{N,i} \mathcal{V}_{S_{r_i}}(t),\\
{}^{\mathbb{CPC}}\mathfrak{D}^{\alpha}_{0,t} E_r(t) &= \frac{A_N}{t^{\alpha-1}}\left[Q^{\alpha}(1-\alpha) E_r(t) + \alpha Q^{1-\alpha} C^{2\alpha} E'_r(t)\right] - \sum_{i=1}^{N} t^{1-\alpha-i} B_{N,i} \mathcal{V}_{E_{r_i}}(t),\\
{}^{\mathbb{CPC}}\mathfrak{D}^{\alpha}_{0,t} I_r(t) &= \frac{A_N}{t^{\alpha-1}}\left[Q^{\alpha}(1-\alpha) I_r(t) + \alpha Q^{1-\alpha} C^{2\alpha} I'_r(t)\right] - \sum_{i=1}^{N} t^{1-\alpha-i} B_{N,i} \mathcal{V}_{I_{r_i}}(t),
\end{aligned}
$$

and

$$
\begin{aligned}
\mathcal{V}_{S_{h_i}}(t) &= \int_0^t s^{i-1}\left[Q^{\alpha}(1-\alpha) S_h(s) + \alpha Q^{1-\alpha} C^{2\alpha} S'_h(s)\right] ds,\\
\mathcal{V}_{E_{h_i}}(t) &= \int_0^t s^{i-1}\left[Q^{\alpha}(1-\alpha) E_h(s) + \alpha Q^{1-\alpha} C^{2\alpha} E'_h(s)\right] ds,\\
\mathcal{V}_{I_{h_i}}(t) &= \int_0^t s^{i-1}\left[Q^{\alpha}(1-\alpha) I_h(s) + \alpha Q^{1-\alpha} C^{2\alpha} I'_h(s)\right] ds,\\
\mathcal{V}_{C_{h_i}}(t) &= \int_0^t s^{i-1}\left[Q^{\alpha}(1-\alpha) C_h(s) + \alpha Q^{1-\alpha} C^{2\alpha} C'_h(s)\right] ds,\\
\mathcal{V}_{R_{h_i}}(t) &= \int_0^t s^{i-1}\left[Q^{\alpha}(1-\alpha) R_h(s) + \alpha Q^{1-\alpha} C^{2\alpha} R'_h(s)\right] ds,\\
\mathcal{V}_{V_{h_i}}(t) &= \int_0^t s^{i-1}\left[Q^{\alpha}(1-\alpha) V_h(s) + \alpha Q^{1-\alpha} C^{2\alpha} V'_h(s)\right] ds,\\
\mathcal{V}_{S_{r_i}}(t) &= \int_0^t s^{i-1}\left[Q^{\alpha}(1-\alpha) S_r(s) + \alpha Q^{1-\alpha} C^{2\alpha} S'_r(s)\right] ds,\\
\mathcal{V}_{E_{r_i}}(t) &= \int_0^t s^{i-1}\left[Q^{\alpha}(1-\alpha) E_r(s) + \alpha Q^{1-\alpha} C^{2\alpha} E'_r(s)\right] ds,\\
\mathcal{V}_{I_{r_i}}(t) &= \int_0^t s^{i-1}\left[Q^{\alpha}(1-\alpha) I_r(s) + \alpha Q^{1-\alpha} C^{2\alpha} I'_r(s)\right] ds,
\end{aligned}
$$

where A_N and $B_{N,i}$ are given by (6.1) under the conditions

$$
\mathcal{V}'_{S_{h_i}}(t) = t^{i-1}\left[Q^{\alpha}(1-\alpha) S_h(t) + \alpha Q^{1-\alpha} C^{2\alpha} S'_h(t)\right], \quad \mathcal{V}'_{S_{h_i}}(0) = 0, \quad i = 1, \ldots, N,
$$

$$
\begin{aligned}
\mathcal{V}'_{E_{h_i}}(t) &= t^{i-1}\left[Q^{\alpha}(1-\alpha)E_h(t)+\alpha Q^{1-\alpha}C^{2\alpha}E'_h(t)\right], \quad \mathcal{V}'_{E_{h_i}}(0)=0, \quad i=1,\ldots,N,\\
\mathcal{V}'_{I_{h_i}}(t) &= t^{i-1}\left[Q^{\alpha}(1-\alpha)I_h(t)+\alpha Q^{1-\alpha}C^{2\alpha}I'_h(t)\right], \quad \mathcal{V}'_{I_{h_i}}(0)=0, \quad i=1,\ldots,N,\\
\mathcal{V}'_{C_{h_i}}(t) &= t^{i-1}\left[Q^{\alpha}(1-\alpha)C_h(t)+\alpha Q^{1-\alpha}C^{2\alpha}C'_h(t)\right], \quad \mathcal{V}'_{C_{h_i}}(0)=0, \quad i=1,\ldots,N,\\
\mathcal{V}'_{R_{h_i}}(t) &= t^{i-1}\left[Q^{\alpha}(1-\alpha)R_h(t)+\alpha Q^{1-\alpha}C^{2\alpha}R'_h(t)\right], \quad \mathcal{V}'_{R_{h_i}}(0)=0, \quad i=1,\ldots,N,\\
\mathcal{V}'_{V_{h_i}}(t) &= t^{i-1}\left[Q^{\alpha}(1-\alpha)V_h(t)+\alpha Q^{1-\alpha}C^{2\alpha}V'_h(t)\right], \quad \mathcal{V}'_{V_{h_i}}(0)=0, \quad i=1,\ldots,N,\\
\mathcal{V}'_{S_{r_i}}(t) &= t^{i-1}\left[Q^{\alpha}(1-\alpha)S_r(t)+\alpha Q^{1-\alpha}C^{2\alpha}S'_r(t)\right], \quad \mathcal{V}'_{S_{r_i}}(0)=0, \quad i=1,\ldots,N,\\
\mathcal{V}'_{E_{r_i}}(t) &= t^{i-1}\left[Q^{\alpha}(1-\alpha)E_r(t)+\alpha Q^{1-\alpha}C^{2\alpha}E'_r(t)\right], \quad \mathcal{V}'_{E_{r_i}}(0)=0, \quad i=1,\ldots,N,\\
\mathcal{V}'_{I_{r_i}}(t) &= t^{i-1}\left[Q^{\alpha}(1-\alpha)I_r(t)+\alpha Q^{1-\alpha}C^{2\alpha}I'_r(t)\right], \quad \mathcal{V}'_{I_{r_i}}(0)=0, \quad i=1,\ldots,N.
\end{aligned}
$$

7. Results and discussion

This section uses the numerical algorithm from the previous section to obtain the numerical solutions of the $\mathbb{CPC}$-$\mathbb{MPOX}$ model (3.2). The values of the basic parameters are listed as in Table 2 with the initial condition: $S_h(0) = 3.4\times10^8$, $E_h(0) = 1000$, $I_h(0) = 100$, $C_h(0) = 100$, $R_h(0) = 1\times10^6$, $V_h(0) = 1\times10^6$, $S_r(0) = 9\times10^4$, $E_r(0) = 100$, and $I_r(0) = 100$. From the given data, we obtain $\Re_0 = 1.5379\times10^4 > 1, \epsilon_1 = 1.42043, \epsilon_2 = 0.69421, \epsilon_3 = 0.13750, \epsilon_4 = 0.01003, \epsilon_5 = 0.00018, \epsilon_6 = 9.32369\times10^{-9}, \epsilon_7 = 1.03004\times10^{-13}, h_1 = 0.59741, h_2 = 0.00990, h_3 = 9.32362\times10^{-9}, g_1 = 0.11395, g_2 = 0.00018, g_3 = 1.03004\times10^{-13}, d_1 = 0.00896, d_2 = 9.32308\times10^{-9}, e_1 = 0.00018, e_2 = 1.03004\times10^{-13}, f_1 = 9.31797\times10^{-9}$. Consequently, these calculated values satisfy the conditions (i)–(vii) in Theorem 4.5. Thus, the endemic equilibrium point is locally asymptotically stable.

Table 2. The values of parameter used for the simulations of the $\mathbb{CPC}$-$\mathbb{MPOX}$ model (3.2).

Parameter	Value in days	Source	Parameter	Value in days	Source
Λ_h	11731.91	[55]	ω	0.4670	[40]
Λ_r	0.016	[9]	ν	0.0843	[40]
b_1	0.5701	[40]	μ_h	$1/(79\times365)$	[55]
b_2	0.2508	[40]	μ_r	0.000016	[9]
b_3	0.2461	[40]	λ	0.2393	[40]
a_1	0.0486	[40]	η	0.201	[40]
a_2	0.1119	[40]	δ_1	0.0011	[40]
a_3	0.1053	[40]	δ_2	0.00010091	[40]

Here, Figure 2 shows the numerical solutions for the classical $\mathbb{MPOX}$ model (3.1) of each group of human and rodent populations, while Figure 3 expresses the numerical solutions utilizing the $\mathbb{CPC}$ fractional operator for the $\mathbb{CPC}$-$\mathbb{MPOX}$ model (3.2) with varies $\alpha = 0.995, 0.985, 0.975, 0.965, 0.955$. As shown in both of the mentioned figures, the findings demonstrate that the fractional order model follows the same trend as the traditional model but is more flexible and has a higher degree of freedom. At larger fractional orders, increasing and decreasing behavior converges to the classical model more quickly than small fractional orders. Furthermore, from Figure 3 observation, a slight adjustment in the fractional order α was found to cause only a minor change in the behavior. This indicates that variations

in the fractional order have a negligible impact on the stability of the disease dynamics across different groups within the proposed model. In addition, the simulation takes place over a 500-day period. Under certain conditions, solution trajectories in all population groups reach the steady-state for all various values of α as time passes. Figure 2a and Figure 3a indicate the behavior of the susceptible humans. It is observed that the amount of them decreases rapidly in a short time in the beginning and tends to a steady-state as time tends to infinity. Figure 2b, Figure 3b, Figure 2c, Figure 3c, Figure 2d, Figure 3d, Figure 2i, and Figure 3i indicate the behavior of the exposed, infectious, clinically ill humans, and the infected rodents, respectively. We can see that the populations of each group are quite similar in order to gradually increase before reaching a steady state as time passes. Figure 2e and Figure 3e indicate the behavior of the recovered humans, and we extended the period to 5000 days for trend clearly observation. We found that the behavior of this group is increasing and tends to the steady state in the end. The behavior of the vaccinated humans is shown in Figure 2f and Figure 3f, demonstrating rapid population growth in a very short time and then reaching the equilibrium point. The behavior of the susceptible rodents drops initially before tending to a steady state, as seen in Figure 2g and Figure 3g. While Figure 2h and Figure 3h indicate the behavior of the exposed rodents, the population climbs to a peak and then falls until reaching a stable state.

Additionally, we place greater emphasis on examining the influence of the immunity-induced recovery rate ω on the dynamics of three human compartments regarding the $\mathbb{MPOX}$ infection, which are exposed, infectious, and clinically ill individuals. The parameter representing the recovery rate is varied with the following values: 0.4670 (baseline from Table 2), 0.5137 (10% increase), 0.5604 (20% increase), 0.6538 (40% increase), and 0.8406 (80% increase) under vary $\alpha = 1$, 0.9 and 0.8 as seen in Figures 4–6, respectively. These graphs present two significant observations. First, an increase in ω levels corresponds to a clear reduction in the amount of infected individuals across all groups. Second, lower α values lead to a slightly faster decline in the amount of infected humans.

Similarly, investigating the impact of the contact rates between infected individuals or infected rodents on exposed, infected, and clinically ill humans is also highly significant. In this context, the parameter value for the contact rate of infected individuals with the susceptible population is utilized as follows: 0.5701 (baseline from Table 2), 0.62711 (10% increase), 0.68412 (20% increase), 0.79814 (40% increase), and 0.91216 (60% increase). The contact rate of infected rodents with the susceptible population is utilized as follows: 0.2508 (baseline from Table 2), 0.27588 (10% increase), 0.30096 (20% increase), 0.35112 (40% increase), and 0.40128 (60% increase). Figures 7–9 demonstrate the impact of varying contact rate parameters b_1 and b_2 under different values of α: 1, 0.9, and 0.8, respectively. The graphs indicate that the contact rate substantially influences the population sizes of the respective groups. An increase in the contact rate leads to a corresponding increase in the amount of individuals in the groups mentioned. Besides, a reduction in the value of α leads to a slightly faster decline in the population sizes of all groups.

Therefore, based on all of the simulations above in various scenarios, we found a key finding that the fractional order or the memory index, the immunity-induced recovery rate, and the contact rates between infected individuals or infected rodents are factors that play an important role in determining whether monkeypox infection levels increase or decrease in the human population. These parameters can serve as control measures for monkeypox transmission.

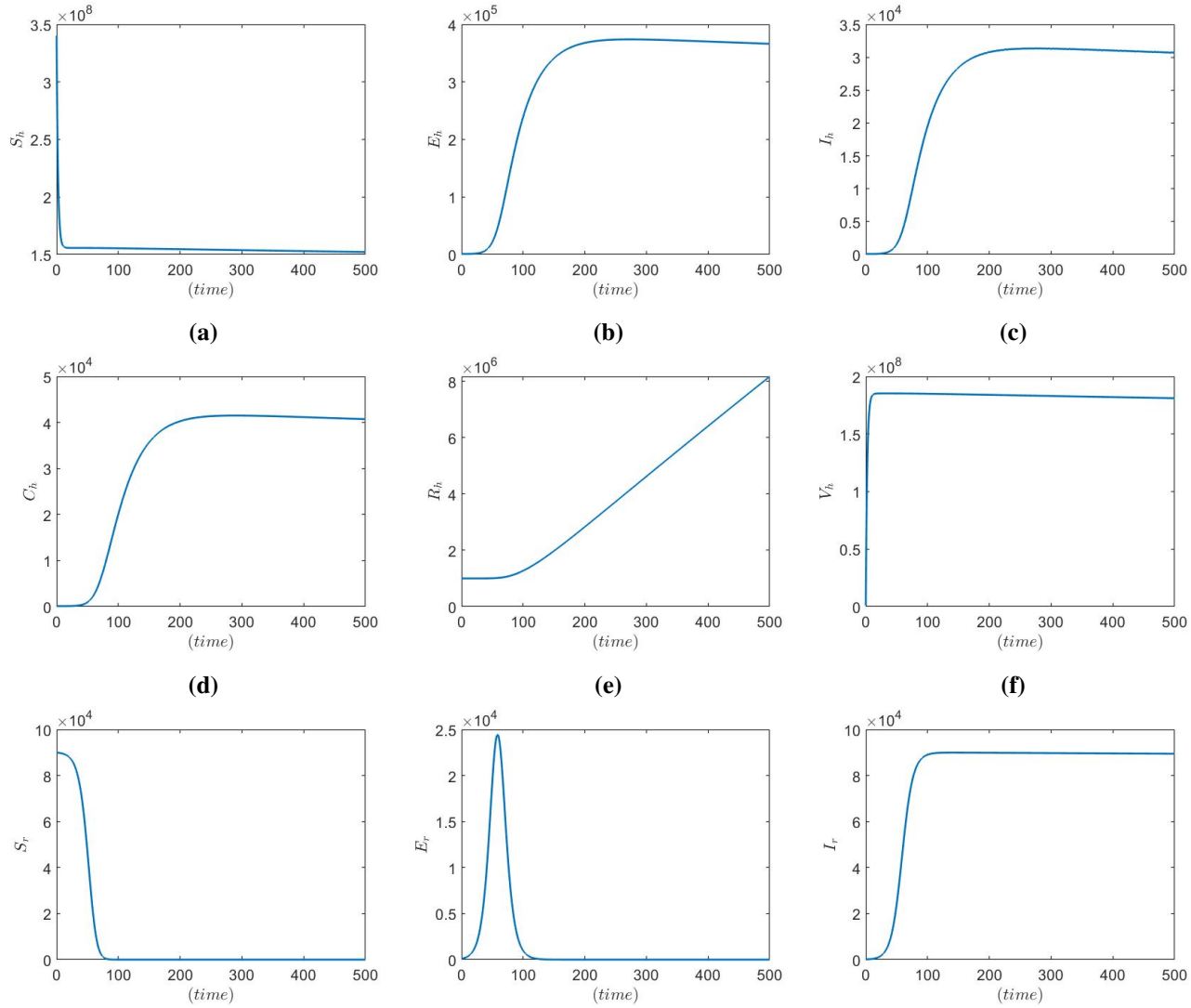

Figure 2. Simulations of $S_h(t)$, $E_h(t)$, $I_h(t)$, $C_h(t)$, $R_h(t)$, $V_h(t)$, $S_r(t)$, $E_r(t)$, and $I_r(t)$ of the ℂℙℂ-𝕄ℙ𝕆𝕏 model (3.2).

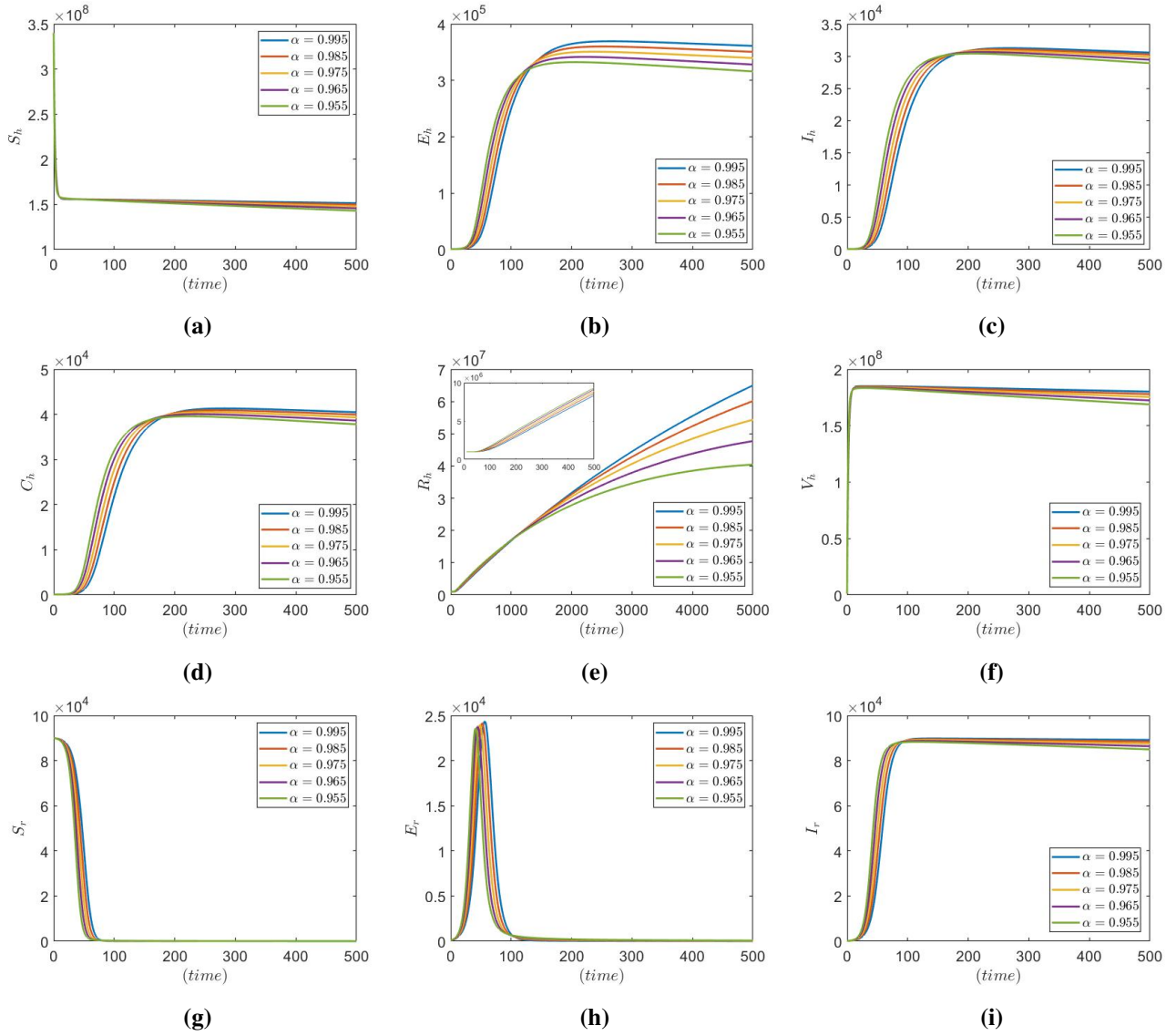

Figure 3. Simulations of $S_h(t)$, $E_h(t)$, $I_h(t)$, $C_h(t)$, $R_h(t)$, $V_h(t)$, $S_r(t)$, $E_r(t)$, and $I_r(t)$ of the $\mathbb{CPC}$-$\mathbb{MPX}$ model (3.2) when $\alpha \in \{0.995, 0.985, 0.975, 0.965, 0.955\}$.

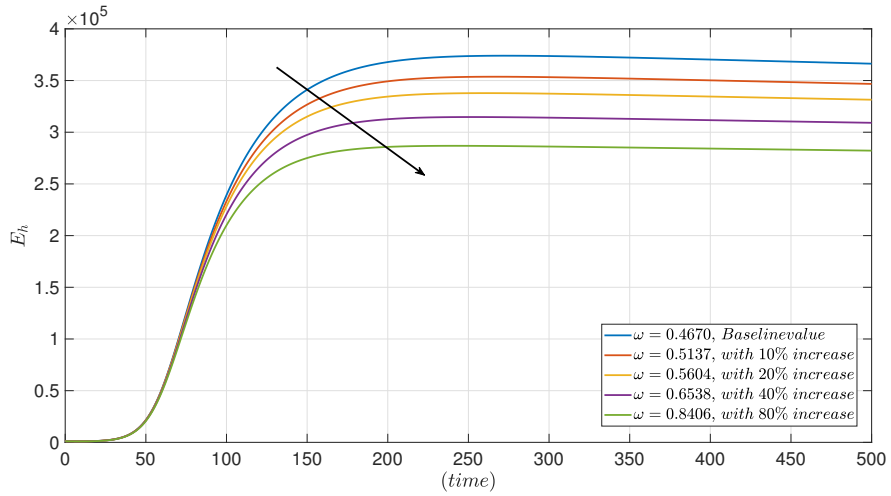

(a)

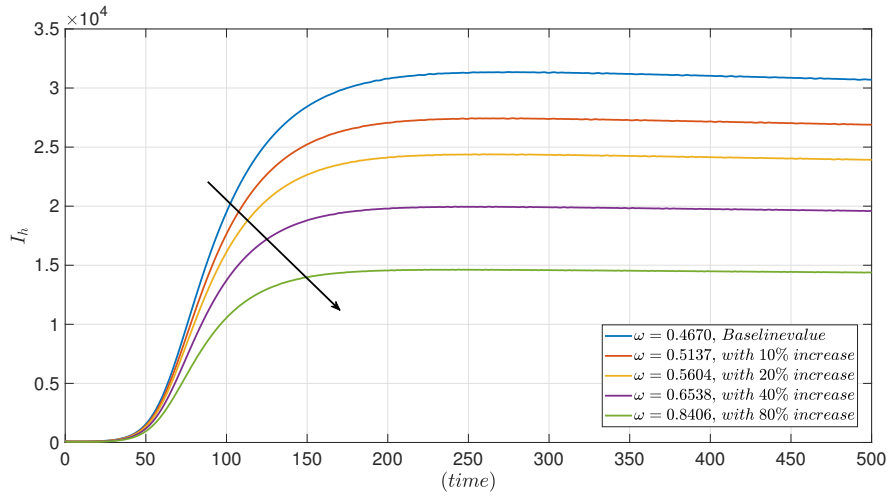

(b)

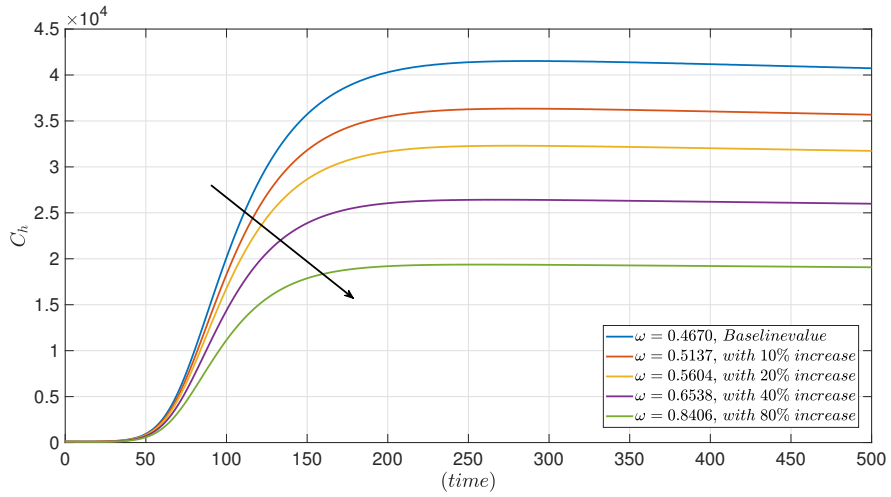

(c)

Figure 4. Impact of recovery rate ω when $\alpha = 1.00$.

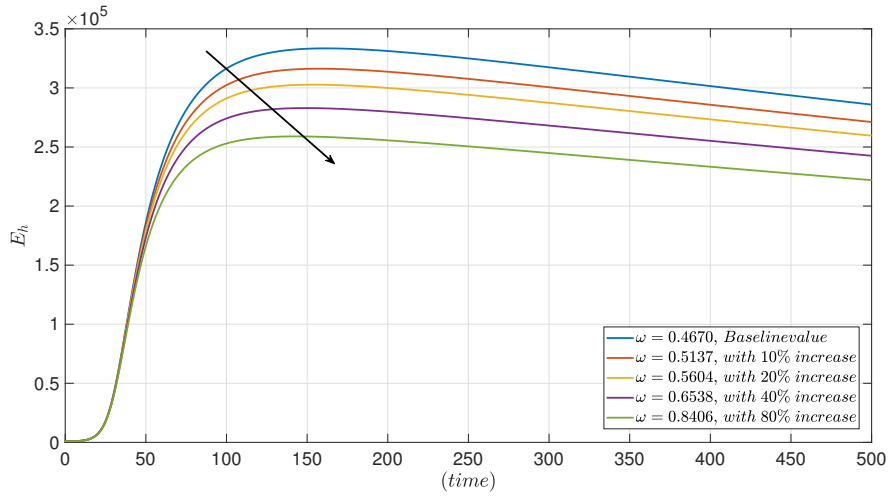

(a)

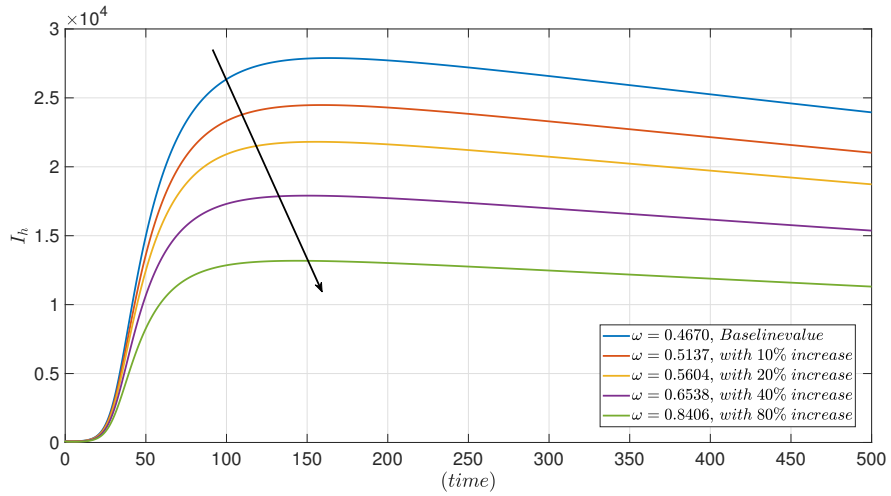

(b)

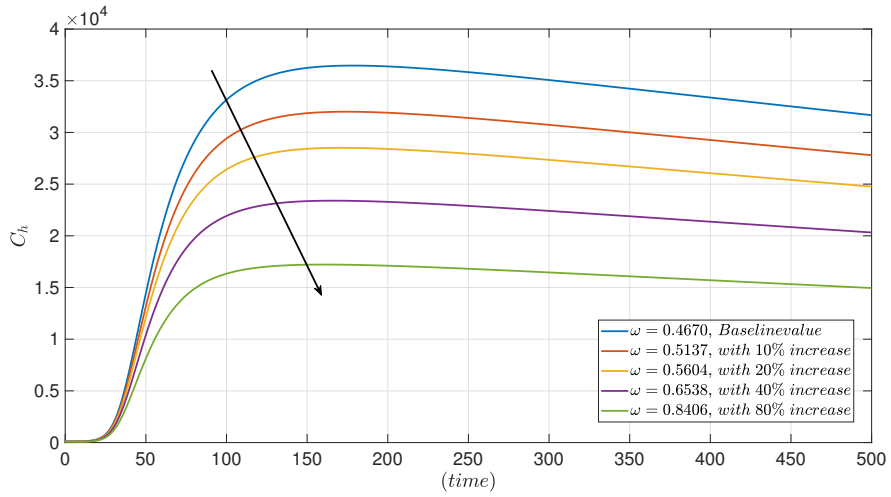

(c)

Figure 5. Effect of recovery rate ω when $\alpha = 0.90$.

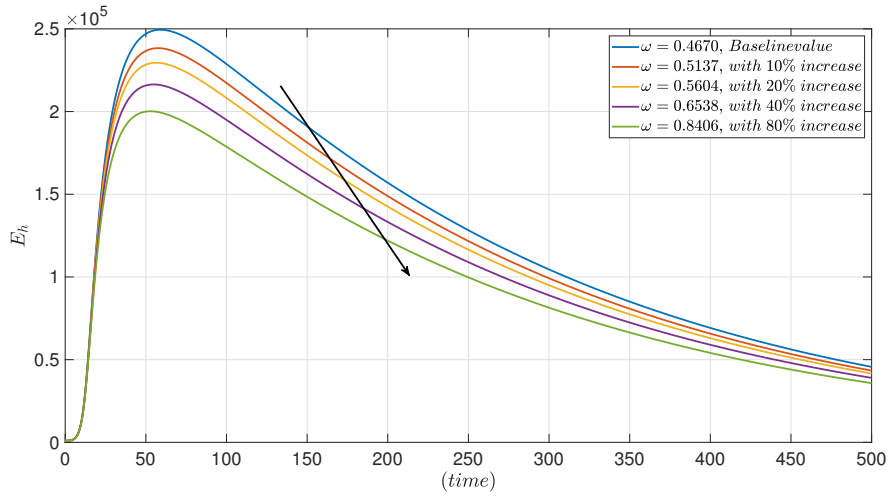

(a)

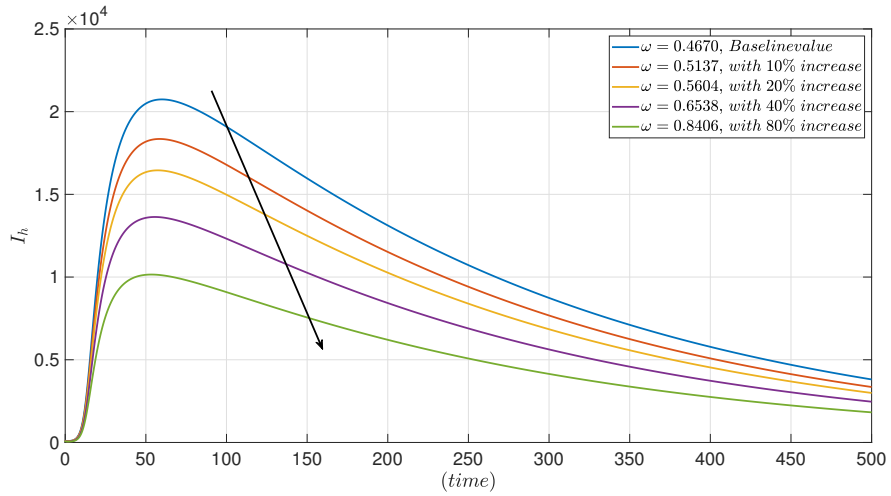

(b)

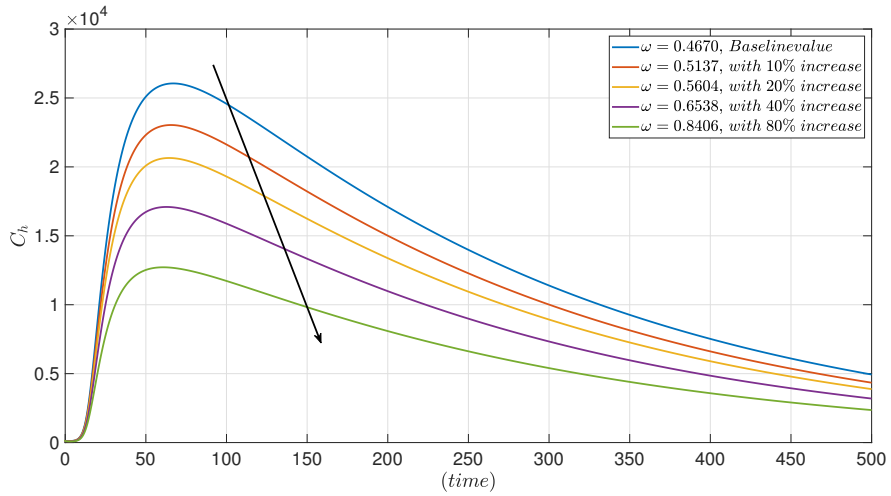

(c)

Figure 6. Effect of recovery rate ω when $\alpha = 0.80$.

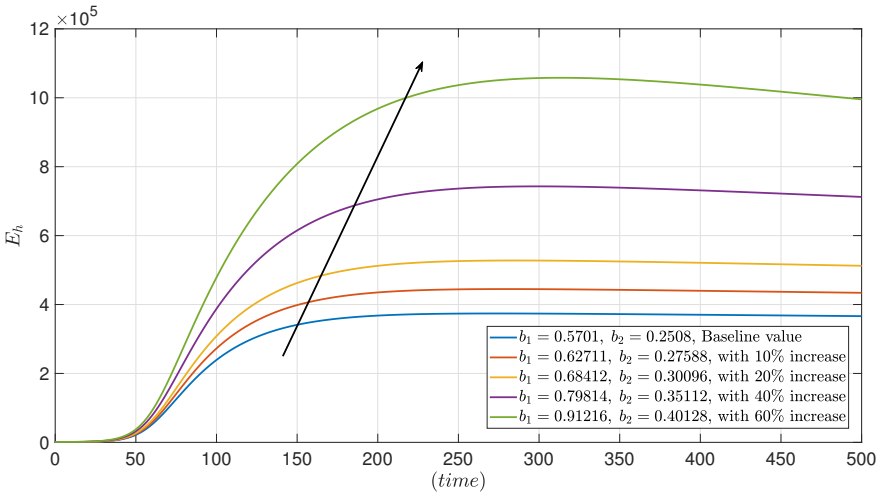

(a)

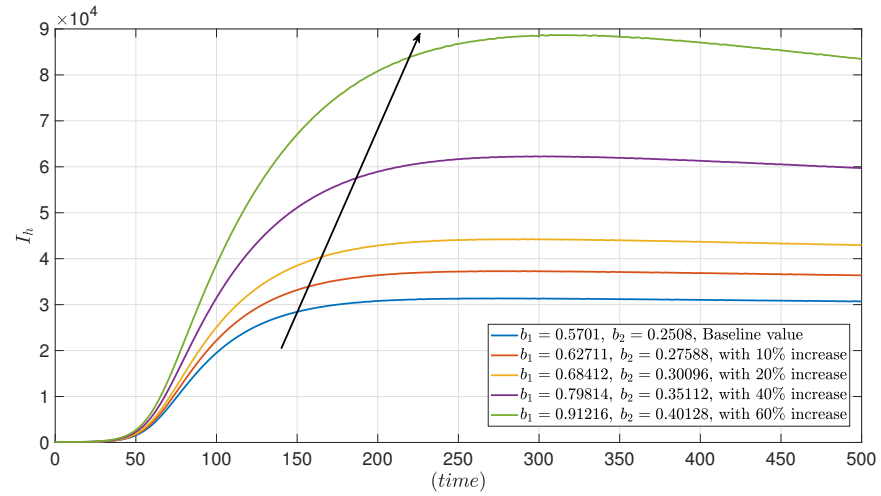

(b)

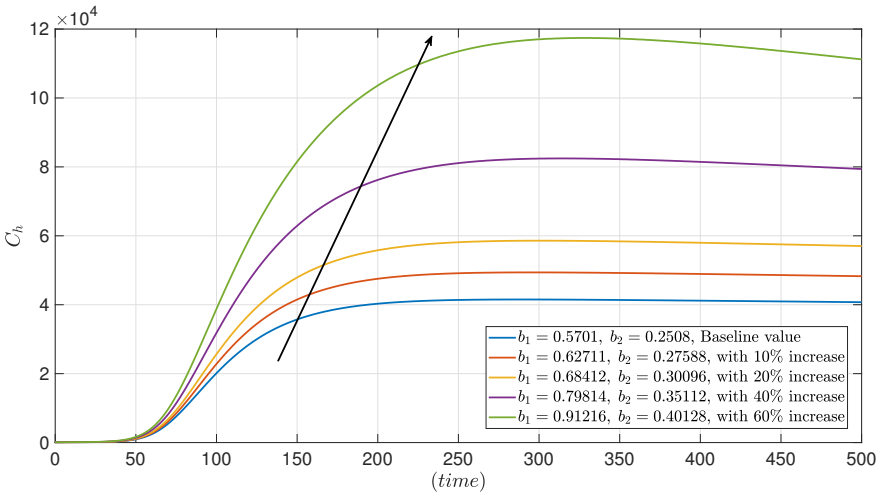

(c)

Figure 7. Effect of infected contact rates b_1 and b_2 when $\alpha = 1.00$.

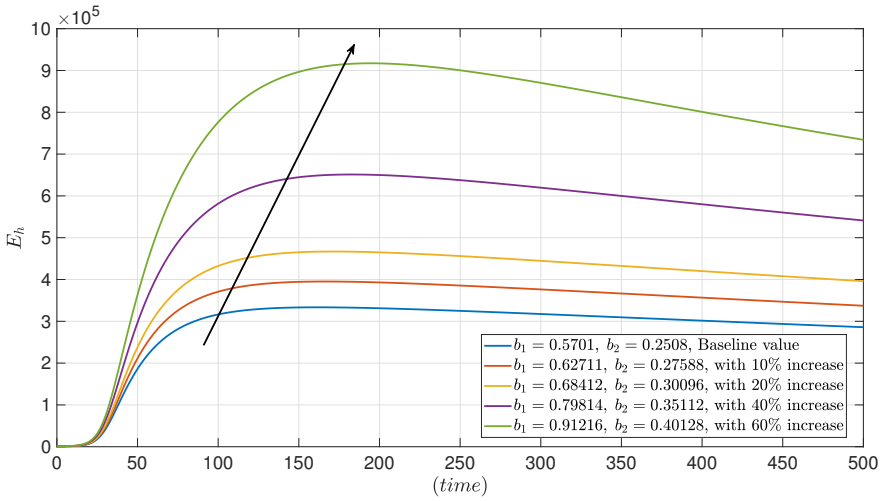

(a)

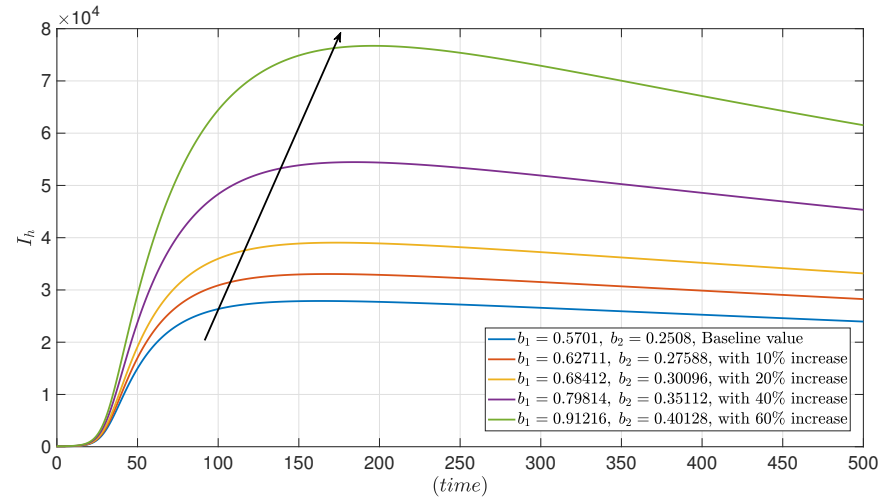

(b)

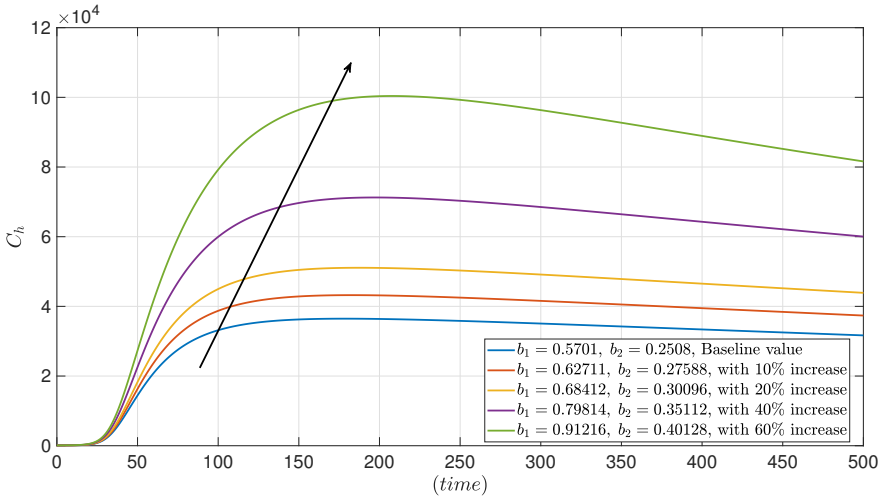

(c)

Figure 8. Effect of infected contact rates b_1 and b_2 when $\alpha = 0.9$.

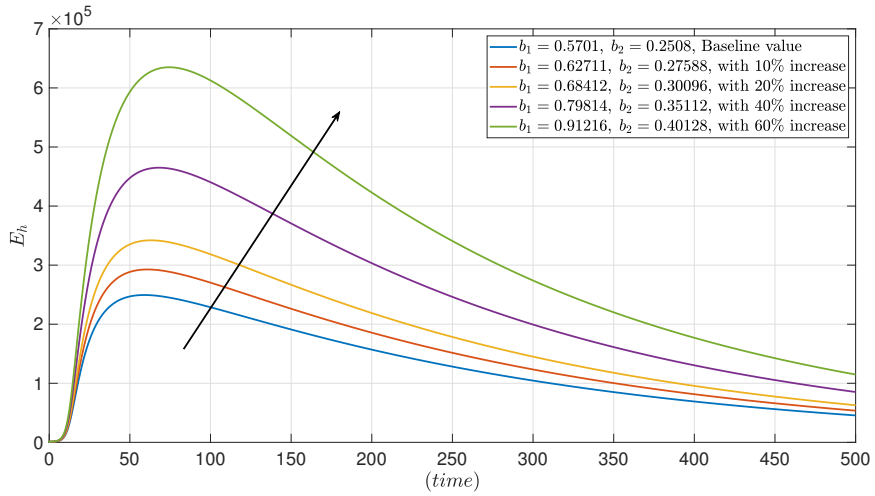

(a)

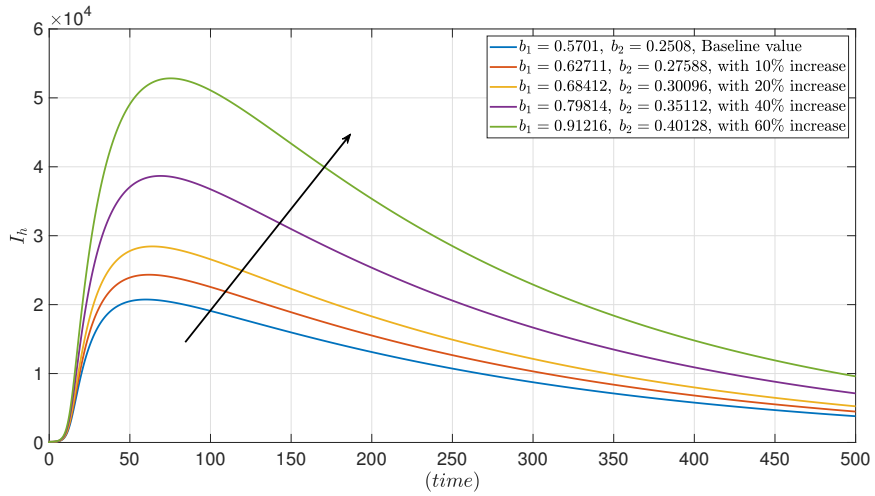

(b)

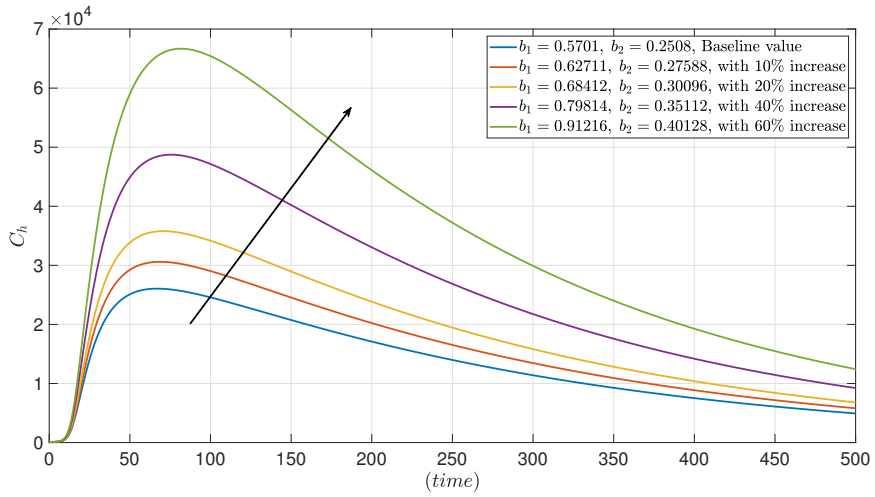

(c)

Figure 9. Effect of infected contact rates b_1 and b_2 when $\alpha = 0.8$.

8. Conclusions

This study presented a $\mathbb{CPC}$ fractional derivative model for the spread of the monkeypox virus, accounting for interactions between humans and rodents. The model was developed to analyze system behavior and identify parameters that can help control the disease. For the theoretical part, we proved the positiveness and boundedness of solutions and examined the equilibrium points and the basic reproduction number. We investigated the local asymptotically stable steady state. We verified the qualitative results of the suggested model, including the existence and uniqueness results, using the Banach contraction mapping principle. Various Ulam's stability was demonstrated to ensure the existing solutions. The exactness of the theoretical guarantee is confirmed via the numerical simulations in all diagrams utilizing a decomposition formula for a constant proportional Caputo derivative. For the numerical and graphical parts, the graphical results highlight the key advantage of our proposed $\mathbb{CPC}$-$\mathbb{MPOX}$ model. It proves to be more realistic and practical than the traditional model, and its flexibility enhances precision, enabling us to achieve superior outcomes compared to the classical approach. Using the value of the parameters in Table 2, it was shown by numeric calculation that $\Re_0 > 1$ and all conditions of Routh-Hurwitz criteria are satisfied. Hence, we concluded that the endemic equilibrium point is locally asymptotically stable, which supports Theorem 4.5. Furthermore, the suggested model is shown by rising the value parameters of the recovery rate due to immunity and the contact rates of susceptible humans with infected humans and infected rodents at various levels and different fractional orders to analyze the effect in population dynamics influenced by the spread of $\mathbb{MPOX}$ via graphical simulation. The study demonstrated that the factors in our case can be incorporated into the control mechanisms of monkeypox transmission. These findings may offer valuable insights into the prevention and control of $\mathbb{MPOX}$ outbreaks in the future.

For future work, applying the $\mathbb{CPC}$ derivatives operator to study and analyze other epidemic models in real-world situations can be a proper alternative technique. On the other hand, other fractional operators, such as piece-wise and stochastic operators, can be considered for $\mathbb{MPOX}$ virus transmission to investigate real-world situations more realistically.

Author contributions

Jutarat Kongson: Conceptualization, Methodology, Writing-original draft, Writing-review & editing, Formal analysis, Funding acquisition; Chatthai Thaiprayoon: Conceptualization, Methodology, Writing–original draft, Writing–review & editing, Software, Supervision; Weerawat Sudsutad: Conceptualization, Methodology, Writing-original draft, Writing-review & editing, Formal analysis. All authors have read and agreed to the published version of the manuscript.

Use of Generative-AI tools declaration

The authors declare they have not used Artificial Intelligence (AI) tools in creating this article.

Acknowledgments

J. Kongson (jutarat_k@go.buu.ac.th) and C. Thaiprayoon (chatthai@go.buu.ac.th) would like to thank Burapha University for providing bench space and support.

Funding

This work was financially supported by (i) Burapha University (BUU), (ii) Thailand Science Research and Innovation (TSRI), and (iii) National Science Research and Innovation Fund (NSRF) (Fundamental Fund: Grant no. 75/2567).

Conflict of interest

The authors declare no conflict of interest.

References

1. World Health Organization, Monkeypox outbreak 2022, World Health Organization, 2022. Available from: https://www.who.int/emergencies/situations/monkeypox-oubreak-2022.
2. S. Jayswal, J. Kakadiya, A narrative review of pox: smallpox vs monkeypox, *The Egyptian Journal of Internal Medicine*, **34** (2022), 90. http://doi.org/10.1186/s43162-022-00174-0
3. Z. Jezek, F. Fenner, *Human monkeypox*, New York: Karger, 1988.
4. S. Essbauer, M. Pfeffer, H. Meyer, Zoonotic poxviruses, *Vet. Microbiol.*, **140** (2010), 229–236. https://doi.org/10.1016/j.vetmic.2009.08.026
5. A. W. Rimoin, P. M. Mulembakani, S. C. Johnston, J. O. L. Smith, N. K. Kisalu, T. L. Kinkela, et al., Major increase in human monkeypox incidence 30 years after smallpox vaccination campaigns cease in the Democratic Republic of Congo, *Proc. Natl. Acad. Sci.*, **107** (2010), 16262–16267. https://doi.org/10.1073/pnas.1005769107
6. S. Usman, I. I. Adamu, Modeling the transmission dynamics of the monkeypox virus infection with treatment and vaccination interventions, *Journal of Applied Mathematics and Physics*, **5** (2017), 2335–2353. https://doi.org/10.4236/jamp.2017.512191
7. A. Elsonbaty, W. Adel, A. Aldurayhim, A. El-Mesady, Mathematical modeling and analysis of a novel monkeypox virus spread integrating imperfect vaccination and nonlinear incidence rates, *Ain Shams Eng. J.*, **15** (2024), 102451. https://doi.org/10.1016/j.asej.2023.102451
8. S. A. Somma, N. I. Akinwande, U. D. Chado, A mathematical model of monkeypox virus transmission dynamics, *Ife Journal of Science*, **21** (2019), 195–204. https://doi.org/10.4314/ijs.v21i1.17
9. O. J. Peter, S. Kumar, N. Kumari, F. A. Oguntolu, K. Oshinubi, R. Musa, Transmission dynamics of monkeypox virus: a mathematical modelling approach, *Model. Earth Syst. Environ.*, **8** (2022), 3423–3434. https://doi.org/10.1007/s40808-021-01313-2

10. O. J. Peter, C. E. Madubueze, M. M. Ojo, F. A. Oguntolu, T. A. Ayoola, Modeling and optimal control of monkeypox with cost-effective strategies, *Model. Earth Syst. Environ.*, **9** (2023), 1989–2007. https://doi.org/10.1007/s40808-022-01607-z

11. O. J. Peter, A. Abidemi, M. M. Ojo, T. A. Ayoola, Mathematical model and analysis of monkeypox with control strategies, *Eur. Phys. J. Plus*, **138** (2023), 242. https://doi.org/10.1140/epjp/s13360-023-03865-x

12. C. P. Bhunu, S. Mushayabasa, Modelling the transmission dynamics of pox-like infections, *IAENG International Journal of Applied Mathematics*, **41** (2011), 141–149.

13. L. E. Depero, E. Bontempi, Comparing the spreading characteristics of monkeypox (MPX) and COVID-19: insights from a quantitative model, *Environ. Res.*, **235** (2023), 116521. https://doi.org/10.1016/j.envres.2023.116521

14. N. Z. Alshahrani, F. Alzahrani, A. M. Alarifi, M. R. Algethami , M. N. Alhumam, H. A. M. Ayied, et al., Assessment of knowledge of monkeypox viral infection among the general population in Saudi Arabia, *Pathogens*, **11** (2022), 904. https://doi.org/10.3390/pathogens11080904

15. D. Baleanu, A. Fernandez, On fractional operators and their classifications, *Mathematics*, **7** (2019), 830. https://doi.org/10.3390/math7090830

16. K. Diethelm, *The analysis of fractional differential equations: an application-oriented exposition using differential operators of Caputo type*, Berlin: Springer, 2010. https://doi.org/10.1007/978-3-642-14574-2

17. U. N. Katugampola, New approach to a generalized fractional integral, *Appl. Math. Comput.*, **218** (2011), 860–865. https://doi.org/10.1016/j.amc.2011.03.062

18. A. Atangana, D. Baleanu, New fractional derivatives with nonlocal and non-singular kernel, theory, and application to heat transfer model, *Therm. Sci.*, **20** (2016), 763–769. https://doi.org/10.2298/TSCI160111018A

19. A. Atangana, Fractal-fractional differentiation and integration: connecting fractal calculus and fractional calculus to predict complex system, *Chaos Soliton. Fract.*, **102** (2017), 396–406. https://doi.org/10.1016/j.chaos.2017.04.027

20. R. Kamocki, A new representation formula for the Hilfer fractional derivative and its application, *J. Comput. Appl. Math.*, **308** (2016), 39–45. https://doi.org/10.1016/j.cam.2016.05.014

21. D. Baleanu, A. Fernandez, A. Akgül, On a fractional operator combining proportional and classical differintegrals, *Mathematics*, **8** (2020), 360. https://doi.org/10.3390/math8030360

22. W. Sudsutad, J. Kongson, C. Thaiprayoon, On generalized (k,ψ)-Hilfer proportional fractional operator and its applications to the higher-order Cauchy problem, *Bound. Value Probl.*, **2024** (2024), 83. https://doi.org/10.1186/s13661-024-01891-x

23. N. H. Sweilam, S. M. Al-Mekhlafi, D. Baleanu, A hybrid fractional optimal control for a novel Coronavirus (2019-nCov) mathematical model, *J. Adv. Res.*, **32** (2021), 149–160. https://doi.org/10.1016/j.jare.2020.08.006

24. H. Gnerhan, H. Dutta, M. A. Dokuyucu, W. Adel, Analysis of a fractional HIV model with Caputo and constant proportional Caputo operators, *Chaos Soliton. Fract.*, **139** (2020), 110053. https://doi.org/10.1016/j.chaos.2020.110053

25. M. Farman, A. Shehzad, A. Akgül, D. Baleanu, M. D. la Sen, Modelling and analysis of a measles epidemic model with the constant proportional Caputo operator, *Symmetry*, **15** (2023), 468. https://doi.org/10.3390/sym15020468

26. M. Farman, C. Alfiniyah, A constant proportional caputo operator for modeling childhood disease epidemics, *Decision Analytics Journal*, **10** (2024), 100393. https://doi.org/10.1016/j.dajour.2023.100393

27. M. Arif, P. Kumam, W. Watthayu, Analysis of constant proportional Caputo operator on the unsteady Oldroyd-B fluid flow with Newtonian heating and non-uniform temperature, *Z. Angew. Math. Mech.*, **104** (2024), e202300048. https://doi.org/10.1002/zamm.202300048

28. A. El-Mesady, O. J. Peter, A. Omame, F. A. Oguntolu, Mathematical analysis of a novel fractional order vaccination model for Tuberculosis incorporating susceptible class with underlying ailment, *Int. J. Model. Simul.*, in press. https://doi.org/10.1080/02286203.2024.2371684

29. O. J. Peter, N. D. Fahrani, Fatmawati, Windarto, C. W. Chukwu, A fractional derivative modeling study for measles infection with double dose vaccination, *Healthcare Analytics*, **4** (2023), 100231. https://doi.org/10.1016/j.health.2023.100231

30. O. J. Peter, A. Yusuf, M. M. Ojo, S. Kumar, N. Kumari, F. A. Oguntolu, A mathematical model analysis of meningitis with treatment and vaccination in fractional derivatives, *Int. J. Appl. Comput. Math.*, **8** (2022), 117. https://doi.org/10.1007/s40819-022-01317-1

31. O. J. Peter, A. Yusuf, K. Oshinubi, F. A. Oguntolu, J. O. Lawal, A. I. Abioye, et al., Fractional order of pneumococcal pneumonia infection model with Caputo Fabrizio operator, *Results Phys.*, **29** (2021), 104581. https://doi.org/10.1016/j.rinp.2021.104581

32. O. J. Peter, Transmission dynamics of fractional order brucellosis model using Caputo-Fabrizio operator, *Int. J. Differ. Equat.*, **2020** (2020), 2791380. https://doi.org/10.1155/2020/2791380

33. O. J. Peter, F. A. Oguntolu, M. M. Ojo, A. O. Oyeniyi, R. Jan, I. Khan, Fractional order mathematical model of monkeypox transmission dynamics, *Phys. Scr.*, **97** (2022), 084005. https://doi.org/10.1088/1402-4896/ac7ebc

34. M. Ngungu, E. Addai, A. Adeniji, U. M. Adam, K. Oshinubi, Mathematical epidemiological modeling and analysis of monkeypox dynamism with non-pharmaceutical intervention using real data from United Kingdom, *Front. Public Health*, **11** (2023), 1101436. https://doi.org/10.3389/fpubh.2023.1101436

35. F. A. Wireko, I. K. Adu, C. Sebil, J. K. K. Asamoah, A fractal-fractional order model for exploring the dynamics of Monkeypox disease, *Decision Analytics Journal*, **8** (2023), 100300. https://doi.org/10.1016/j.dajour.2023.100300

36. W. Sudsutad, C. Thaiprayoon, J. Kongson, W. Sae-Dan, A mathematical model for fractal-fractional monkeypox disease and its application to real data, *AIMS Math.*, **9** (2024), 8516–8563. https://doi.org/10.3934/math.2024414

37. A. El-Mesady, A. Elsonbaty, W. Adel, On nonlinear dynamics of a fractional order monkeypox virus model, *Chaos Soliton. Fract.*, **164** (2022), 112716. https://doi.org/10.1016/j.chaos.2022.112716

38. M. A. Qurashi, S. Rashid, A. M. Alshehri, F. Jarad, F. Safdar, New numerical dynamics of the fractional monkeypox virus model transmission pertaining to nonsingular kernels, *Mathematical Biosciences and Engineering*, **20** (2022), 402–436. https://doi.org/10.3934/mbe.2023019

39. N. Zhang, E. Addai, L. Zhang, M. Ngungu, E. Marinda, J. K. K. Asamoah, Fractional modeling and numerical simulation for unfolding marburg-monkeypox virus co-infection transmission, *Fractals*, **31** (2023), 2350086. https://doi.org/10.1142/S0218348X2350086X

40. B. Liu, S. Farid, S. Ullah, M. Altanji, R. Nawaz, S. W. Teklu, Mathematical assessment of monkeypox disease with the impact of vaccination using a fractional epidemiological modeling approach, *Sci. Rep.*, **13** (2023), 13550. https://doi.org/10.1038/s41598-023-40745-x

41. A. S. Biswas, B. H. Aslam, P. K. Tiwari, Mathematical modeling of a novel fractional-order monkeypox model using the Atangana-Baleanu derivative, *Phys. Fluids*, **35** (2023), 117130. https://doi.org/10.1063/5.0174767

42. S. Okyere, J. Ackora-Prah, Modeling and analysis of monkeypox disease using fractional derivatives, *Results Eng.*, **17** (2023), 100786. https://doi.org/10.1016/j.rineng.2022.100786

43. A. Atangana, S. I. Araz, *New numerical scheme with Newton polynomial: theory, methods, and applications*, 1 Eds., Elsevier, 2021. https://doi.org/10.1016/C2020-0-02711-8

44. V. S. Erturk, P. Kumar, Solution of a COVID-19 model via new generalized Caputo-type fractional derivatives, *Chaos Soliton. Fract.*, **139** (2020), 110280. https://doi.org/10.1016/j.chaos.2020.110280

45. H. Najafi, S. Etemad, N. Patanarapeelert, J. K. K. Asamoah, S. Rezapour, T. Sitthiwirattham, A study on dynamics of CD4+ T-cells under the effect of HIV-1 infection based on a mathematical fractal-fractional model via the Adams-Bashforth scheme and Newton polynomials, *Mathematics*, **10** (2022), 1366. https://doi.org/10.3390/math10091366

46. D. Boucenna, D. Baleanu, A. B. Makhloufd, A. M. Nagy, Analysis and numerical solution of the generalized proportional fractional Cauchy problem, *Appl. Numer. Math.*, **167** (2021), 173–186. https://doi.org/10.1016/j.apnum.2021.04.015

47. W. Sudsutad, C. Thaiprayoon, A. Aphithana, J. Kongson, W. Sae-Dan, Qualitative results and numerical approximations of the (k,ψ)-Caputo proportional fractional differential equations and applications to blood alcohol levels model, *AIMS Math.*, **9** (2024), 34013–34041. https://doi.org/10.3934/math.20241622

48. S. M. Ulam, *A collection of mathematical problems*, New York: Interscience, 1960.

49. D. H. Hyers, On the stability of the linear functional equation, *Proc. Natl. Acad. Sci.*, **27** (1941), 222–224. https://doi.org/10.1073/pnas.27.4.222

50. T. M. Rassias, On the stability of linear mappings in Banach spaces, *Proc. Amer. Math. Soc.*, **72** (1978), 297–300. https://doi.org/10.1090/S0002-9939-1978-0507327-1

51. J. Wang, X. Li, E_α-Ulam type stability of fractional order ordinary differential equations, *J. Appl. Math. Comput.*, **45** (2014), 449–459. https://doi.org/10.1007/s12190-013-0731-8

52. I. Podlubny, *Fractional differential equations*, New York: Academic Press, 1999.

53. G. O. Fosu, E. Akweittey, A. S. Albert, Next-generation matrices and basic reproductive numbers for all phases of the coronavirus disease, *Open J. Math. Sci.*, **4** (2020), 261–272. https://doi.org/10.2139/ssrn.3595958

54. A. Granas, J. Dugundji, *Fixed point theory*, New York: Springer, 2003. https://doi.org/10.1007/978-0-387-21593-8

55. Worldometer, United States population (accessed Nov 2022), Worldometer, 2022. Available from: `https://www.worldometers.info/world-population/us-population/`.